

PHASE TRANSITIONS OF PHOSPHOLIPID MONOLAYERS ON AIR-WATER INTERFACES

by

Christopher Roland

A thesis submitted to the
Faculty of Graduate Studies and Research
in partial fulfillment of the
requirements for the
degree of Master of Science

**Department of Physics
McGill University
Montreal, Quebec, Canada**

 **March 1986**

DEDICATED TO MY PARENTS.

Abstract

We present a model for the π -A isotherms of PC lipid monolayers on an air-water interface. Our model is an Ising-like N-state lattice model solved in the Bethe approximation. It is based on the following ideas:

- (i) The LC/LB transition is a chain disordering transition in which the hydrocarbon chains go from a rigid, all-trans to a chain melted, excited chain configuration. The transition is modified through the growth of finite-sized lipid domains in the LC phase.
- (ii) In the LB phase, the monolayer expands through the introduction of vacancies and the collapse of lipid chains onto the aqueous substrate.
- (iii) The LB/SG transition is a first-order transition driven by the polar head interaction.

We model the LC/LB transition for a system of impure monolayers. The phase transition is shifted, scaled and eliminated.

Résumé

Nous présentons un modèle décrivant les isothermes N-A des monocouches lipidiques PC à une interface air-eau. Notre modèle de type Ising à N-états, est solutionné dans l'approximation de Bethe et se fonde sur les idées suivantes:

- (i) La transition LC/LE est une transition impliquant un désorganisation dans la chaîne d'hydrocarbure qui passe d'un état tout-très, rigide à un état excité, en fusion. La transition est modifiée par le biais de la croissance de domaines finis dans la phase LC.
- (ii) Dans la phase LE, la monocouche se dilate par suite de l'introduction de sites vacants et l'effondrement des chaînes lipidiques dans le substrat aqueux.
- (iii) La transition LE/SG, est une transition d'ordre un, dont l'origine est l'interaction des têtes polaires.

Nous proposons aussi un modèle de la transition LC/LE pour un système de monocouches impures. La transition de phase est décalée, étalée et éliminée.

Acknowledgements

I wish, first and foremost, to thank Dr. M.J.Zuckermann, my supervisor and Dr. A.Georgallas . Without their interest, encouragement and constant help, this work would not have been possible. I wish to thank Ian Graham for advice, friendship and many useful discussions; Mr. Popov for help with the diagrams: Mrs. H.Carinci and Dr. M.Sutton for help with the word processor and to Amir Khadir and Ait Ouwalli for translating the abstract. My thanks also to all the students and staff who have made my sojourn at McGill very pleasant.

Finally, I would like to thank NSERC for two years of financial support.

TABLE OF CONTENTS

	PAGE
ABSTRACT	i
RESUME	ii
ACKNOWLEDGEMENTS	iii
TABLE OF CONTENTS	iv,v
CHAPTER I. LIPID MONOLAYERS AND THEIR PROPERTIES	1
CHAPTER II. THE LIQUID CONDENSED TO LIQUID EXPANDED TRANSITION	11
(i) Order of Phase Transitions	11
(ii) Chain Melting Model	13
(iii) Chain Melting Model With Finite Size Effects	19
CHAPTER III. THE LIQUID-EXPANDED TO SURFACE-GAS TRANSITION	25
(i) Experimental Results	25
(ii) Lattice Gas Models	26
(iii) Lattice Gas Model With Chain Collapse	29
(iv) A Model For Complete π -A Isotherms	39
CHAPTER IV. RESULTS FOR THE COMPLETE MODEL	42
CHAPTER V. LC LE PHASE TRANSITION FOR IMPURE MONOLAYERS	57
(i) Model For Impure Monolayer	57
(ii) Model 1	60
(iii) Results For Model 1	62

(iv) Model II	64
(v) Results for Model II	71
CHAPTER VI. CONCLUSIONS	77
APPENDIX I	81
REFERENCES	92

CHAPTER ONE: LIPID MONOLAYERS AND THEIR PROPERTIES

Phase transitions in quasi-two-dimensional monolayers of amphiphilic molecules have been studied for a variety of lipid systems. Such systems are interesting not only from a thermodynamic viewpoint, but also through the central role which they play in interface science⁽¹⁾.

In the field of membrane biology, studies of monolayer systems may have relevance as possible model systems for some biological membranes^(2,3). Lipid bilayers are now considered to form the underlying matrix of a cell membrane, in which the proteins and other intrinsic molecules are embedded. Furthermore, there is ample evidence of both a theoretical and experimental nature which suggests that lipid bilayers consist of two weakly coupled, back to back monolayers^(4,5). Thus, the study of monolayer properties may well shed light upon phenomena such as the transport of molecules across membrane boundaries, membrane structure and cellular adaptation - all of which may well be related to phase changes in biomembranes^(6,7).

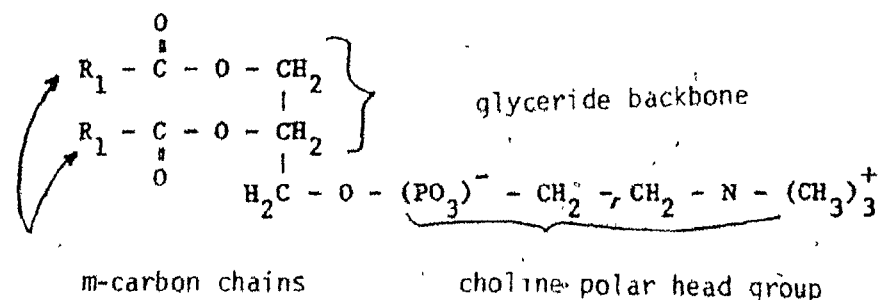
Lipid monolayers occur naturally in lungs, mayonnaise, and soaps. A variety of diverse technical applications for monolayers includes surfactants (e.g. soaps), foodstuffs (e.g. pharmaceuticals, dyes), lubricants, evaporation control, environmental technology, semiconductor devices and the manufacture of biocompatible materials^(8,9).

Amphiphilic molecules consist of two parts, each of which separately have very different solubilities in water. As a prototype, we

can think of an n-chain fatty acid $\text{CH}_3(\text{CH}_2)_n\text{COOH}$. The polar part (COOH group) is very soluble ; the alkane chain, $\text{CH}_3(\text{CH}_2)_n$, insoluble.

We will focus specifically on monolayers of phospholipids with choline polar head groups, notably dipalmitoylphosphatidylcholine (DPPC). Such lipids have two saturated hydrocarbon chains consisting of m - carbon atoms, a glyceride backbone and a hydrophilic phosphatidylcholine head group^(6,7).

Fig.(1.1) - Structure of PC Phospholipid



As the lipid molecules are spread onto the water surface, the hydrocarbon chains are squeezed out of the aqueous substrate because of the strong hydrophobic interaction which results from the high self-attraction of water. The polar head group stays well anchored inside the water surface. As a result, we have the formation of a quasi-two-dimensional monomolecular film^(10,11).

The Langmuir trough (described below) allows one to measure the lateral pressure (Π) and to calculate the area available to each molecule (A). The resultant $\Pi \cdot A$ isotherms exhibit phase behavior very

much like that of a three-dimensional pressure-volume system. In fig.(1.2) we have a typical set of isotherms. At least three phases may be readily identified :

(i) a liquid-condensed (LC) phase with areas per chain being less than 23 \AA^2 .

(ii) a liquid-expanded (LE) phase with areas per chain being roughly between $34\text{--}60 \text{ \AA}^2$.

(iii) a surface gas (SG) or vapour phase with areas per chains being greater than 90 \AA^2 ⁽¹⁴⁾.

The surface gas, found at very low densities and low pressures (about 0.01 dynes/cm. for DPPC and 0.1 dynes/cm. for pentadecanoic acid both at about 25°C) converges onto the isotherms generated by a two-dimensional ideal gas:

$$[1-1] \quad \Pi A = NkT$$

There is probably little or no interaction between different molecules in this region of the isotherms. It is thought that most chains are arranged parallel to the interface^(13,15).

Compression of this film results in the LE/SG phase transition. The observed coexistence region is asymmetrically shaped and is characterized by its extreme range in areas per molecule, running from about a hundred to several thousand angstroms squared. The transition is first-order with its thermodynamic functions obeying mean-field exponent

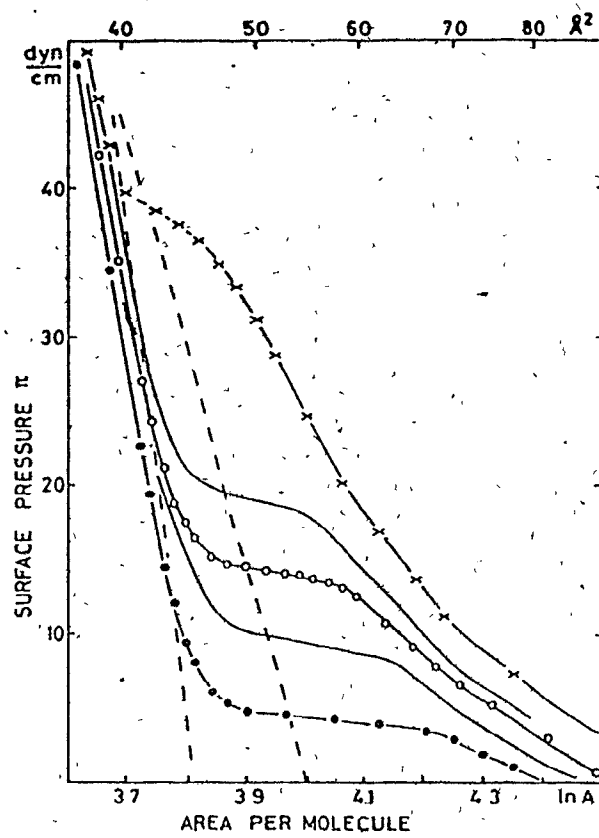


Fig. 1.2 (a) Lateral Pressure - Molecular Area isotherms for DPPC.
The temperatures for the isotherms are 20.4, 27.5, 30,
and 37.5° C. The dotted lines mark the beginning
and the end of the LC phase⁽⁴²⁾.

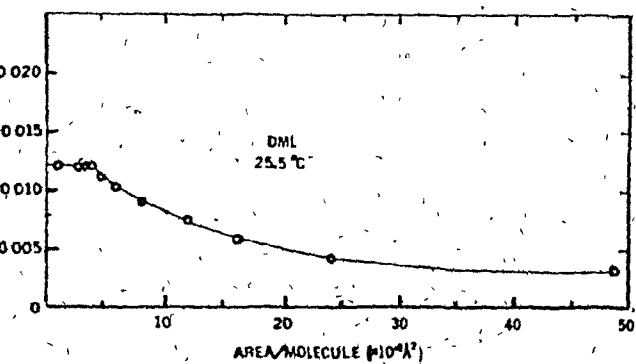
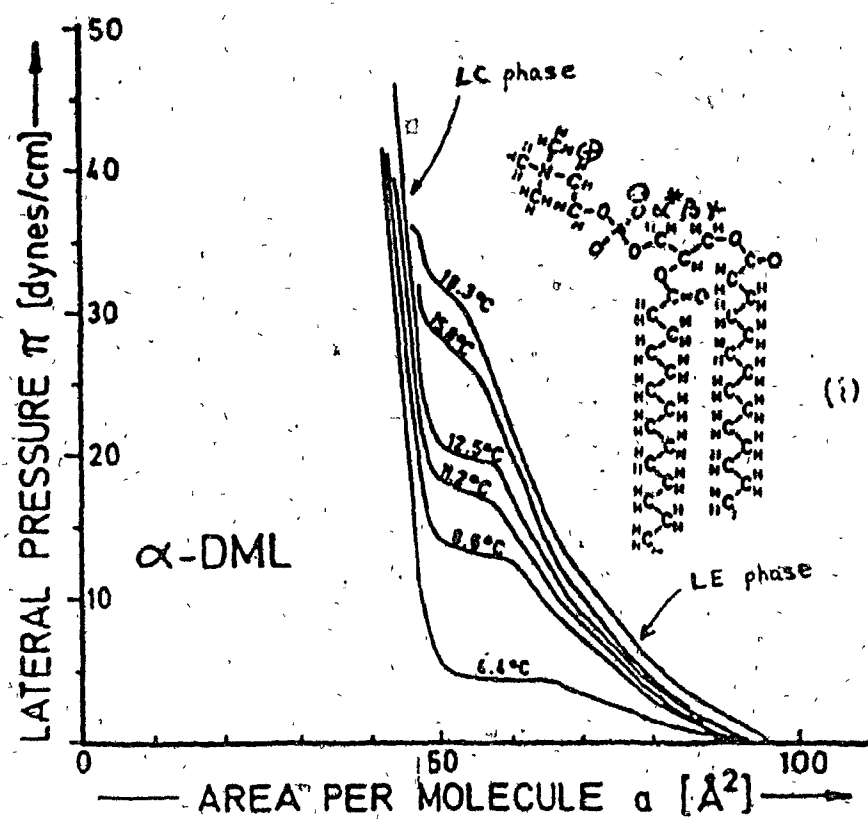


Fig. 1.2 (b) Lateral Pressure - Molecular Area isotherms for α -DML.
 (i) experimental results for LC/LE transition⁽¹²⁾.
 (ii) experimental results for LE/SG transition⁽¹³⁾.

laws. The critical temperature is difficult to determine experimentally due to the possible extrusion of surface-active contaminants from the Langmuir trough. It is estimated to range between 26-40°C (15-18).

The LE phase covers a large range in pressures and exhibits liquid-like behavior. In this phase, the hydrocarbon chains are being more vertically oriented with respect to the interface.

The LC/LE phase transition is characterized by significant non-zero slopes in the coexistence region, and a discontinuous change of slope at the onset of the LE phase. Hysteresis is observed if the film is alternately compressed and expanded (12,19).

The resultant LC phase may be viewed as a semisolid or gel phase. The chains are tightly packed in an all-trans state (this will be clarified later) and vertical with respect to the substrate. Further compression of the film beyond its minimum area per molecule (20.4 Å²/chain for straight chain carboxylic acids) results in the collapse of the monomolecular film. The film folds up onto itself forming three-dimensional multilayer structures (15) (see fig.(1.3)).

Most monolayer experiments measuring the Π -A isotherms are performed with a Langmuir trough (fig.(1.4)). Typically the trough has dimensions 60x15x2 cm.³ and is made out of either teflon or fused silica. To form the monolayer, the surfactant under study, which is insoluble in water, is first dissolved in an organic solvent. The solution is then spread onto the water surface. The organic solvent is

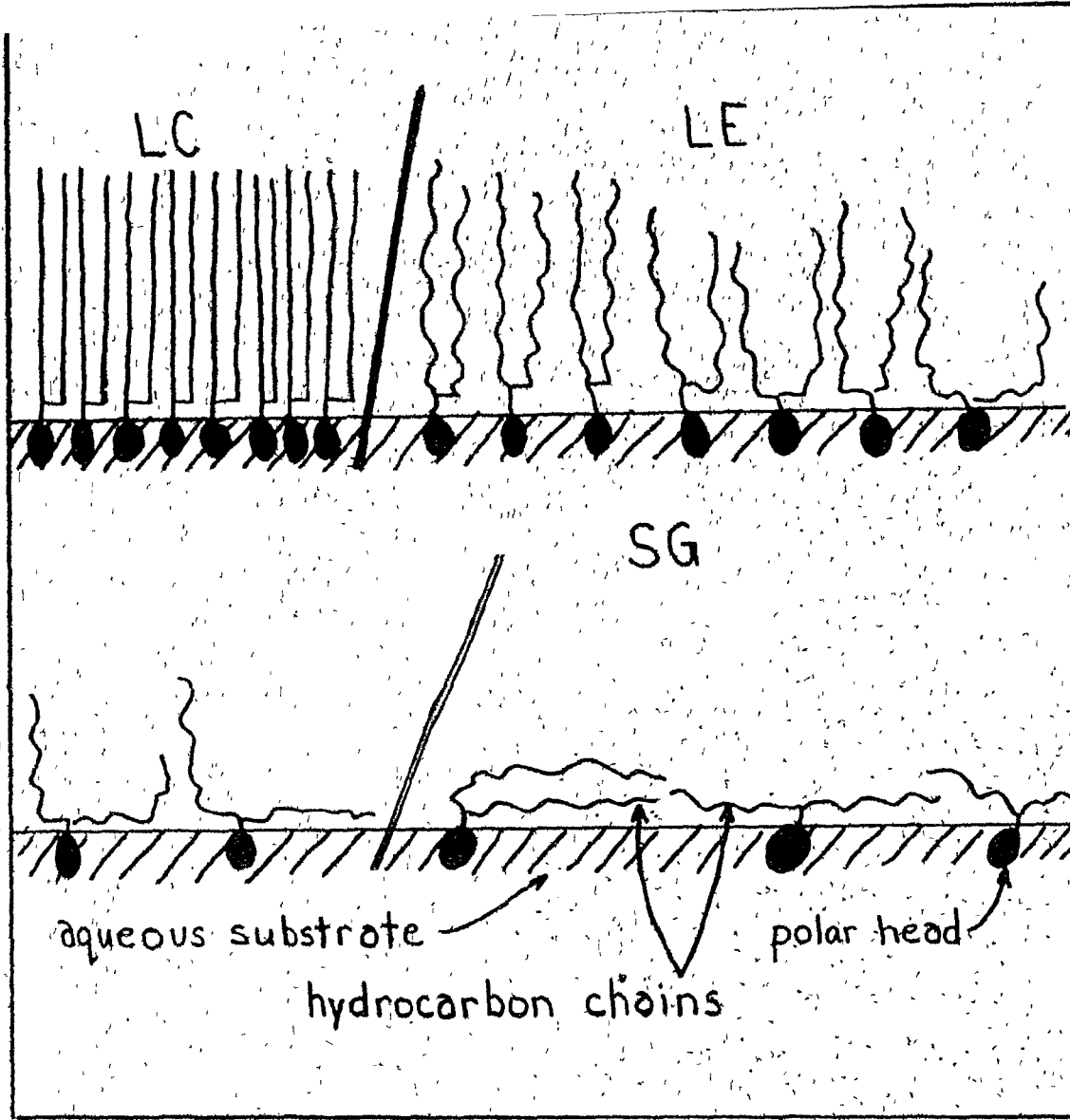
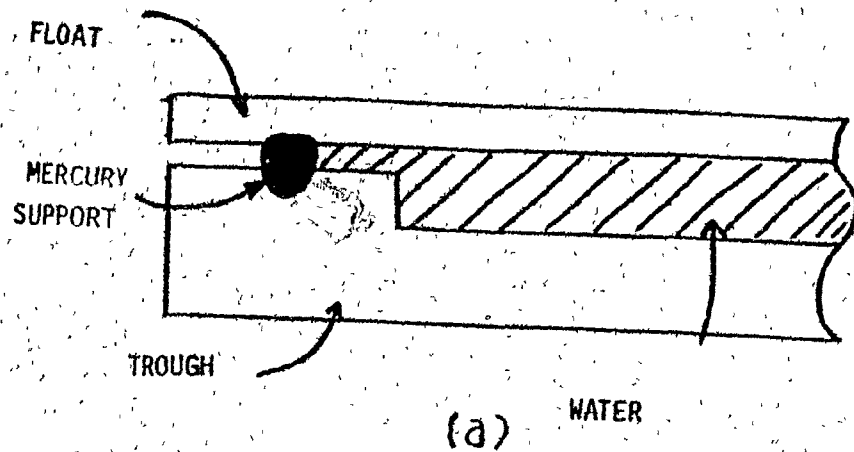
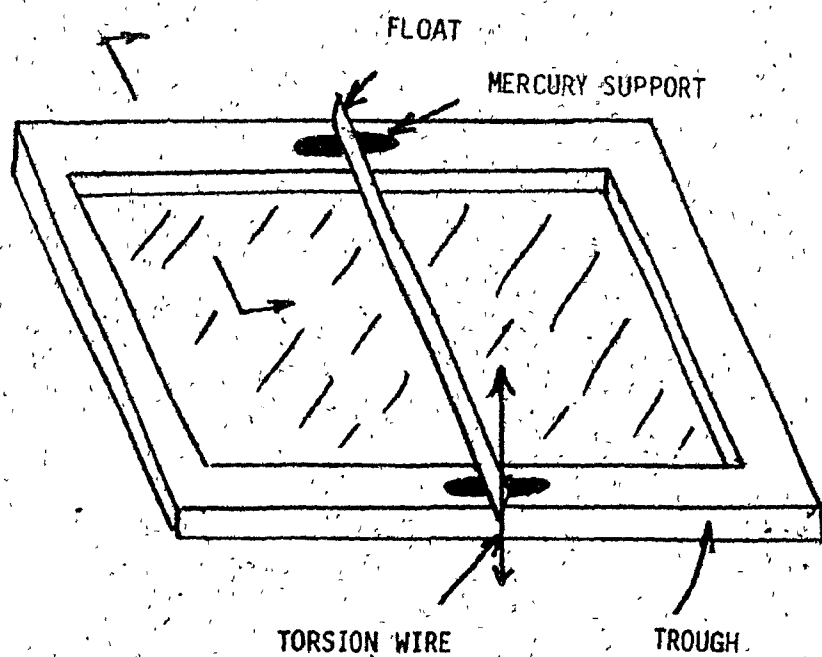


Fig.(I.3) Qualitative picture of the phase changes of phospholipid monolayers . In the LC phase , the lipids are tightly packed in an all-trans configuration . In the LE phase , the chains are disordered and begin to collapse . In the SG phase , most of the chains lie parallel on the substrate . There will be many holes or vacancies .



(a)



(b)

Fig.(1.4) Langmuir trough (a) side view (b) top view

allowed to evaporate, leaving behind a monolayer film, which may then be compressed or expanded with the aid of a movable float. This float serves to confine the surfactant molecules to one end of the trough. It is free to swing along the water surface in response to the film pressure and it acts like a two-dimensional piston. Compression (expansion) takes place at rates sufficiently slow as to maintain equilibrium states at all times. Typical rates of compression are less than 1 \AA^2 per molecule per minute⁽¹⁷⁾.

The lateral pressure is determined as a function of area per molecule through a measurement of the difference in the surface tension between the aqueous substrate (γ_0) and the film (γ):

$$[1.2] \quad \Pi = \gamma_0 - \gamma$$

This is accomplished with the aid of a torsion wire attached to the movable float.

Of interest are also experimental studies of surfactants with a variety of impurities. The films are formed by first spreading the surfactant on preformed substrates containing impurities at predetermined concentrations^(20,21).

It is one of the aims of this thesis to present a model for the phase transitions of phospholipid monolayers with choline headgroups at an air-water interface. Specifically we will model the LC/LB and the LE/SG phase transitions. Our model is an Ising-like N-state lattice.

model with short range interactions. We account for the disordering of hydrocarbon chains, the growth of non-interacting domains in the LC phase, the addition of free volume or holes, and the "lifting up" of the acyl chains in the LE phase. Our model will be solved in the Bethe approximation. We will also present a model for the LC/LE phase transition of the lipid system with substitutional impurities.

In chapter II we present the model of Georgallas and Pink for the LC/LE phase transition. We consider the question of the 'order' of the phase transition and discuss results. This transition is understood in terms of a melting together of domains as the chain configuration changes from an all-trans to a more disordered state.

In chapter III, the model for the LE/SG transition is given. After reviewing the experimental data for the transition, a lattice gas model is presented. The results of this model are given and discussed in the chapter IV.

In chapter V we deal with the effect of adding substitutional impurities to the pure lipid system on the LC/LE phase transition. In chapter VI, we present the conclusions.

CHAPTER 2: THE LIQUID CONDENSED TO LIQUID EXPANDED TRANSITION

This chapter deals explicitly with the theory of the LC/LE phase transition. After briefly reviewing the question of the order of the phase transition, the theory for the LC/LE transition as developed by Georgallas and Pink (GP) (22,27) is presented. The transition is understood in terms of an increase in the number of gauche conformers in the acyl chains of the amphiphilic molecules (a "chain melting" transition) and through the growth of finite-sized, non-interacting domains in the LC phase.

(1) ORDER OF PHASE TRANSITIONS

The experimental Π vs. A isotherms for the LC/LE phase transition show two important characteristics: significant non-zero slopes in the 'coexistence region' and a discontinuous change in slope at the onset of the LE phase⁽¹²⁾. This has lead to questions as to the true nature of the LC/LE phase transition, i.e. whether it is a first-order phase transition, a "diffuse" first-order transition or something else⁽²²⁾?

According to Ehrenfest's criterion, the order of the phase transition is generally indicated by the order of the derivative of the Gibbs free energy (G) at constant temperature (T) in which a discontinuity occurs. Thus, a first-order phase transition is characterized by a discontinuity in the first derivative of the Gibbs free energy. The two-dimensional Clausius-Clapeyron equation :

$$(2-1) \quad \frac{d\Pi}{dT} = \frac{\Delta H}{T\Delta A}$$

relates the change in the surface pressure with temperature to the change in latent heat (ΔH) and the change in area per molecule (ΔA) across the first-order phase transition⁽²³⁾. Phase separation and a well-defined coexistence region are associated with a first-order transition. The LE/SG transition which is discussed in the next chapter is of this type. In a true second-order phase transition, the entropy, enthalpy, and area changes are all zero. However singularities occur in the heat capacity and the isothermal compressibility.

As stated above, there has in fact been a considerable body of controversy about the order of the LC/LE phase transition. The absence of a flat part of the isotherm representing a tie line has prompted several authors to postulate a second-order phase transition. This has been the subject of theoretical models involving both complex chemical structures and renormalization group calculations⁽⁴³⁾.

The model of GP, as used in the present thesis, predicts a first-order phase transition whose tie line is reduced in length due to the effect of domain formation in the transition region. Experimental evidence for the order of the transition is provided by the recent microfluorescence experiments of McConnell et al.⁽⁴⁴⁾. The experiments involve the use of amphiphilic dye molecules which are soluble in the LE phase, but are ejected from the LC phase. The results show explicitly that LC regions nucleate and grow in the transition region as the

pressure increases. We feel that this can be interpreted in terms of very long lived metastable states related to a first-order phase transition. It was originally found that the 'droplet' had a rosette shape indicating the presence of chiral symmetry. However recent experiments by Miller et al.⁽⁴⁵⁾ use pressure jumps to show that in the early growth phase, the droplets are dendritic. This may be due to the presence of dye molecules. Recent work by Mouritsen and Zuckermann describes the phenomena of nucleation and growth in phospholipid monolayers in terms of interfacial melting⁽⁴⁶⁾.

(ii) CHAIN MELTING MODEL

The LC/LE phase transition of lipid monolayers has been variously analyzed in terms of a Landau-Ginzburg theory^(12,24), the effect of excluded volume^(25,26), interacting orientational states⁽¹²⁾ and through the disordering of the hydrocarbon chains via the introduction of gauche bonds. The 'popular' view is that it is the "melting" of the chains which is responsible for the LC/LE phase transition.

Evidence for this comes from x-ray studies of lipid bilayers, which is thought to display an analogous phase transition. At low temperatures, it is found that the hydrocarbon chains form a triangular lattice with lattice constant 4.8 Å between extended and parallel chains. Above the transition, the average intermolecular spacing is 5.3 Å. The diffraction patterns are diffuse, indicating configurational

disorder^(4,10).

In such a model, the effective Hamiltonian may be written in the form :

$$[2-2] \quad \mathcal{H} = \mathcal{H}_{\text{int.}} + \mathcal{H}_{\text{single site}}$$

where $\mathcal{H}_{\text{int.}}$ is the sum of all the short-ranged interactions stabilizing the monolayer film ; $\mathcal{H}_{\text{single site}}$ is the Hamiltonian for a single site, responsible for the disordering within a hydrocarbon chain. The contains contributions from a dipole-dipole interaction between polar head groups and the dispersive van der Waals interaction. The allowed states are chosen in such a way as to disfavour sterically hindered configurations. It is also possible to neglect the dipole-dipole contributions due to the relatively small changes in area taking place^(10,22,27). However, this interaction becomes important (and hence we will include it) as the system undergoes the LE/SG transition.

The disordering of the alkane chains is due to a rotation about any C-C bond of the rest of the chain. For such a rotation, the potential function has three minima : an absolute minimum at $\theta = 0$ and local minima at $\theta_g = \pm 2/3\pi$. For θ_g , the associated energy state lies $\sim 0.45 \times 10^{-13}$ ergs. above the absolute minimum (see Fig.(2.1)).

A theoretical model for the interactions between the hydrocarbon chains must incorporate the vast number of states possible (about 3^{15} for DPPC). To overcome this difficulty, Doniach introduced a two-state

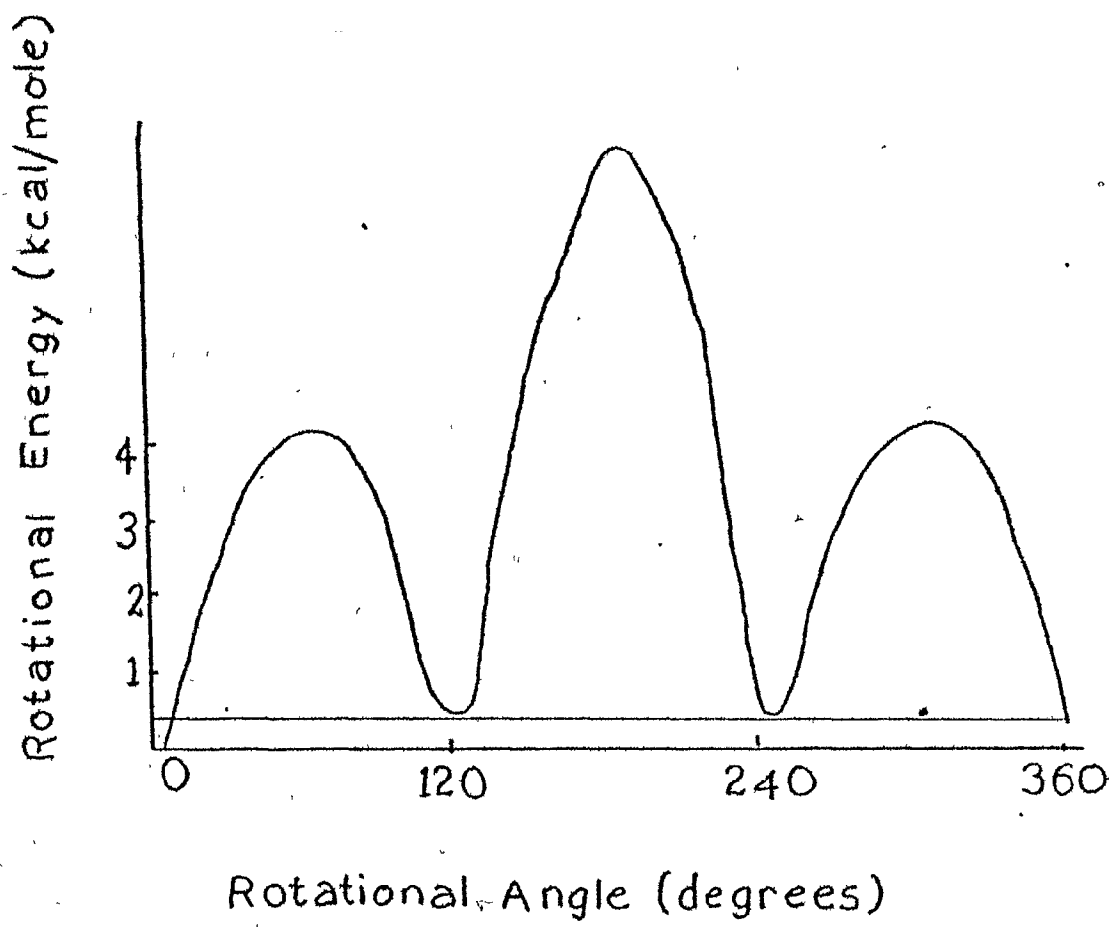
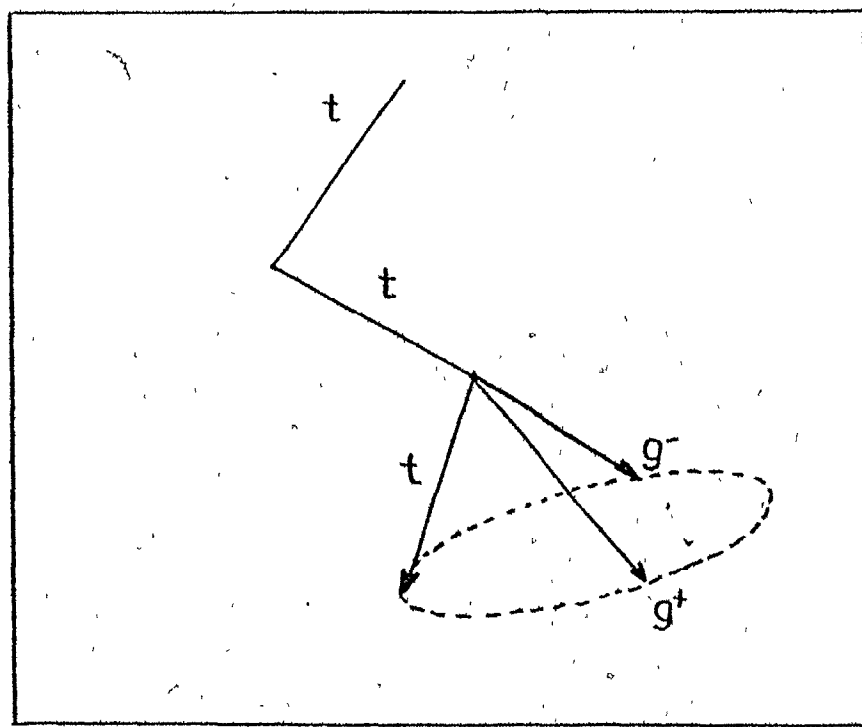


Fig. (2.1)



Configurational states of a C-C bond

model in which the chains would either be in an all-trans ground state (g) or an excited "chain melted" state (e).

The all-trans ground state is taken to have zero internal energy ($E_g = 0$) and degeneracy $D_g = 1$. The lipid chains are fully extended and perpendicular to the substrate projecting an area of $A_g = 20.4 \text{ \AA}^2$ onto the interface^(4,27).

All other physically realistic rotomeric states are included in a highly degenerate state ($D_e \gg 1$) : the excited state. The internal energy E_e includes contributions from the formation of gauche bonds, and to some extent the energy associated with translational motion of the chain. It is the state favoured in the LE phase. It projects a cross-sectional area of $A_e (= 34.0 \text{ \AA}^2)$ onto the interface.

It will further be assumed that each site of a triangular lattice is occupied by a lipid chain. Chains on neighbouring sites will interact via the quadrupole-quadrupole van der Waals interaction^(28,29).

The Hamiltonian for such a model is then written :

$$[2-3] \quad \mathcal{H} = -\frac{J_0}{2} \sum_{\langle ij \rangle} \sum_{n,m} I(n,m) \mathcal{L}_{in} \mathcal{L}_{jm} + \sum_{i,n} (\pi A_n + E_n) \mathcal{L}_{in}$$

where \mathcal{L}_{in} is the projection operator of the lipid chain on the i th. lattice site in state n ; $-J_0 I(n,m)$ is the van der Waals interaction between two nearest neighbour (n.n.) chains ; E_n and A_n denote the effective internal energy and cross-sectional area of the n th. state.

The transformation $\mathcal{L}_{ig} = 1/2(1 + \sigma_1)$ and $\mathcal{L}_{ie} = 1/2(1 - \sigma_1)$ with

$\sigma_i = \pm 1$ maps eq.(2-3) into an Ising model with a temperature dependent field :

$$[2-4] \quad \mathcal{H} = -\frac{J}{2} \sum_{\langle ij \rangle} \sigma_i \sigma_j - H(\Pi, T) \sum_i \sigma_i + \text{constants}$$

where

$$[2-5] \quad J = \frac{q}{4} (I(g,g) - 2I(e,g) + I(e,e))$$

$$[2-6] \quad H(\Pi, T) = h(\Pi) - kT/2 \ln(D_e/D_g)$$

$$[2-7] \quad h(\Pi) = \frac{qJ}{4} (I(g,g) - I(e,e)) + 1/2(A_g - A_e) \\ + 1/2(E_e - E_g)$$

q = coordination number of the lattice

The above Hamiltonian contains constant terms, which we will drop since they will not participate in the calculation of the equation of state.

The order parameter $\langle \sigma \rangle$ is related to the average area/chain (A) through :

$$[2-8] \quad \langle A \rangle = A_g \left(\frac{N_g}{N_e + N_g} \right) + A_e \left(\frac{N_e}{N_e + N_g} \right) \\ = \frac{1}{2} [(A_e + A_g) + \langle \sigma \rangle (A_g - A_e)]$$

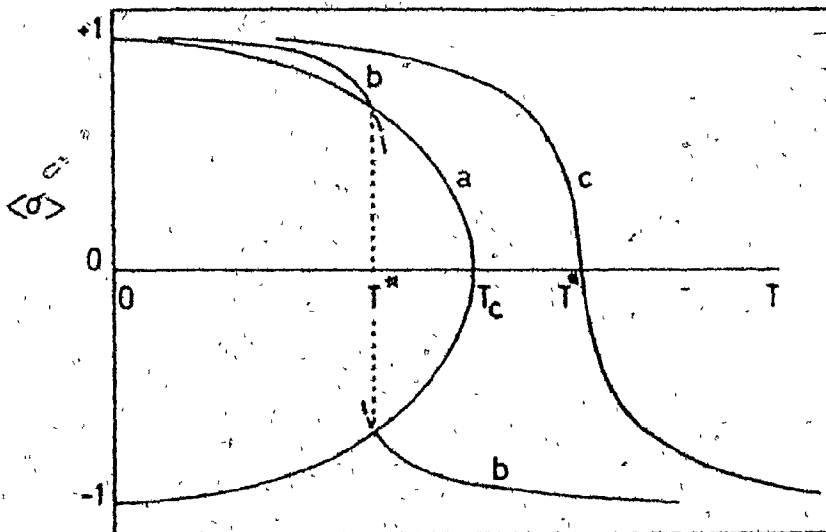
where N_g and N_e denote the number of lipid chains in their ground or excited states respectively.

From eq.(2-6), it is clear that whenever $D_e > D_g$, $H(\Pi, T)$ can change its sign at some temperature T^* and pressure Π^* given when $H(\Pi, T) = 0$:

$$[2.9] \quad T^* = 2h(\Pi^*)/(k \ln(D_e/D_g))$$

The effect of this term is illustrated in fig.(2.2). If $H = 0$, the Hamiltonian (2.4) reduces to the two-dimensional zero-field Ising model. The order parameter corresponding to this model is given by curve (a), with a second-order phase transition at $T=T_c$. If $H > 0$, and small T , the order parameter $\langle\sigma\rangle$, lies near +1 and above the $H = 0$ curve. For large T , $\langle\sigma\rangle$ is near -1 (curve b). If $T^* < T_c$, then H changes sign at T^* resulting in a discontinuous change in $\langle\sigma\rangle$ and a first-order phase transition. If $T^* > T_c$ (curve c), the change can take place continuously.

Fig.(2.2)



The term J in Hamiltonian (2.4) accounts for the van der Waals

interactions between chains. This is the dominant interaction behind the LC/LB phase transition. It has been shown, that for cylinders interacting via the van der Waals forces, one can write as a good approximation⁽³⁰⁾:

$$[2-10] \quad I(n,m) \approx I(n)I(m)$$

where

$$[2-11] \quad I(n) = \sum_p S(\theta_{np}) / \sum_p S(\pi/6) (R_g/R_n)^{5/2}$$

$$[2-12] \quad S(\theta_{np}) = 1/2(3\cos^2(\theta_{np}) - 1)$$

Here θ_{np} represents the angle that the pth. C-C bond of the acyl chain in state n makes with the local axis of symmetry. The ratio R_g/R_n is the ratio between the minimum cylinder radius (R_g) and the radius of the nth. state ($R_n = \sqrt{A_n/\pi}$). $S(\theta_{np})$ is the chain orientational order parameter introduced by Marcelja and Mayer-Saupe⁽²⁹⁾ in the study of liquid crystals. Direct calculations of eqs.(2-9) to (2-13) yields the following values for DPPC : $I(g,g)=1.0$, $I(e,g)=0.148$, $I(e,e)=0.0219$.

Monte-Carlo simulations of the above model on a triangular lattice yields a first-order phase transition with isotherms having a well-defined coexistence curve⁽²⁷⁾.

(iii) CHAIN MELTING MODEL WITH FINITE SIZE EFFECTS

Monte-Carlo simulation of the model described above with the addition of random substitutional impurities yields a transition with

non-zero slopes in the coexistence region. This led to the conjecture by Georgallas and Pink that the LC phase is composed of essentially finite-sized, noninteracting lipid domains. Since an infinite system is necessary for the occurrence of a first-order phase transition⁽²³⁾, these domains must first "melt" or coalesce before the transition can take place. The boundaries of the domains then cease to exist and the system is essentially infinite in size. GP proposed the following ansatz to describe the growth of the domains, each of which contain the same number of molecules N :

$$[2-13] \quad N = N_0 + (N_s - N_0)(1 - \langle \sigma \rangle_N)$$

Here N_0 represents the number of molecules per domain at high pressures in the LC phase ; N_s , at the midpoint of the transition. One expects $N_0 \ll N_s$ since the domains coalesce to form an infinite system.

To date, the two-dimensional Ising model with a field has not been solved analytically and therefore some approximation must be chosen. A further complication is that the effect of the growth of domains must be incorporated into the model. The latter point makes the usual mean-field approximation unsatisfactory, since it will always have a sharp first-order phase transition and a critical point.

The Bethe-Peierls approximation is an improvement over the mean-field approximation since it takes first neighbour correlations into account. To simulate the growth of domains naturally, the model was

solved on a Cayley tree of N sites with $q=6$. A further advantage is that the Hamiltonian (2.4) in the Bethe approximation has an exact solution on the Cayley tree. It possesses a critical point only in the thermodynamic limit of $N \rightarrow \infty$.

The Cayley tree possesses exponential growth - the number of sites is given by :

$$[2-14] \quad N = \begin{cases} \frac{q(q-1)-2}{q-2} & q > 2 \\ 2n+1 & q = 2 \end{cases}$$

where n represents the number of rings on the tree (see fig.(2.3)). The critical temperature exists at $\tanh(J/2kT_c) = 1/(q-1)$. Choosing the critical temperature $T_c = 315^\circ\text{K}$ fixes J_0 to be $\sim 0.972 \times 10^{-13}$ ergs. The difference between the experimentally observed T_c at 304°K is taken to be an artifact of the Bethe approximation. The order parameter is given by :

$$[2-15] \quad \langle \sigma \rangle_N = \frac{z_{N+1} + v z_N}{v + z_N z_{N+1}}$$

$$\frac{z_N}{v} = \frac{(1+u)(1+z_{N-1})^{q-1} - (1-u)(1-z_{N-1})^{q-1}}{(1+u)(1+z_{N-1})^{q-1} + (1-u)(1-z_{N-1})^{q-1}}$$

where

$$v = \tanh(J/kT) \quad u = \tanh(H/kT)$$

Here z_N is a recursion parameter with $z_0 = 0$ ⁽³¹⁾.

It is now possible to solve eqs.(2-4) to (2-16) self-consistently for N and $\langle\sigma\rangle_N$. The free parameters D_e and N_s fix the position of the kink in the LE phase and the slope of the LC phase respectively. Values of $N_s = 10^2$, $N_0 = 10^{10}$, and $D_e = 1275000$ were chosen to obtain the best fit to the $T = 26.1^\circ\text{C}$ isotherm reported by Albrecht et al.. These values correspond to $n = 14$ rings on the Cayley tree and represent a domain enclosing about 400 lipid molecules.

As shown in Fig.(2.4), the model reproduces qualitatively all the features of the LC/LE phase transition. Recently there has been some verification of the growth of finite-sized domains in the LC phase by Fischer and Sackmann , who observed a "spider's web of elongated 100 Å wide cracks " and platelets of $1 \mu\text{m}$ diameter using electron microscopy⁽³²⁾.

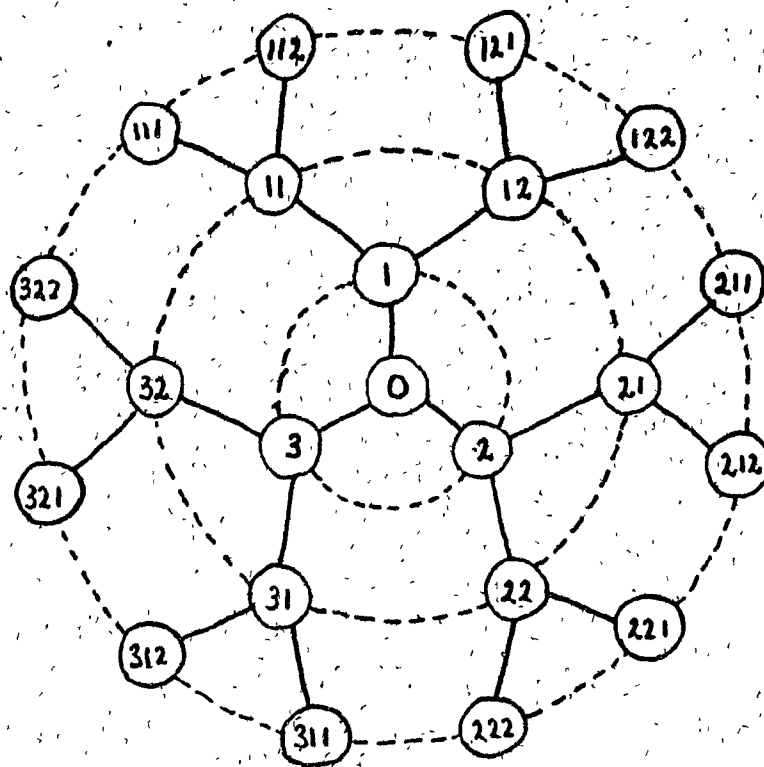
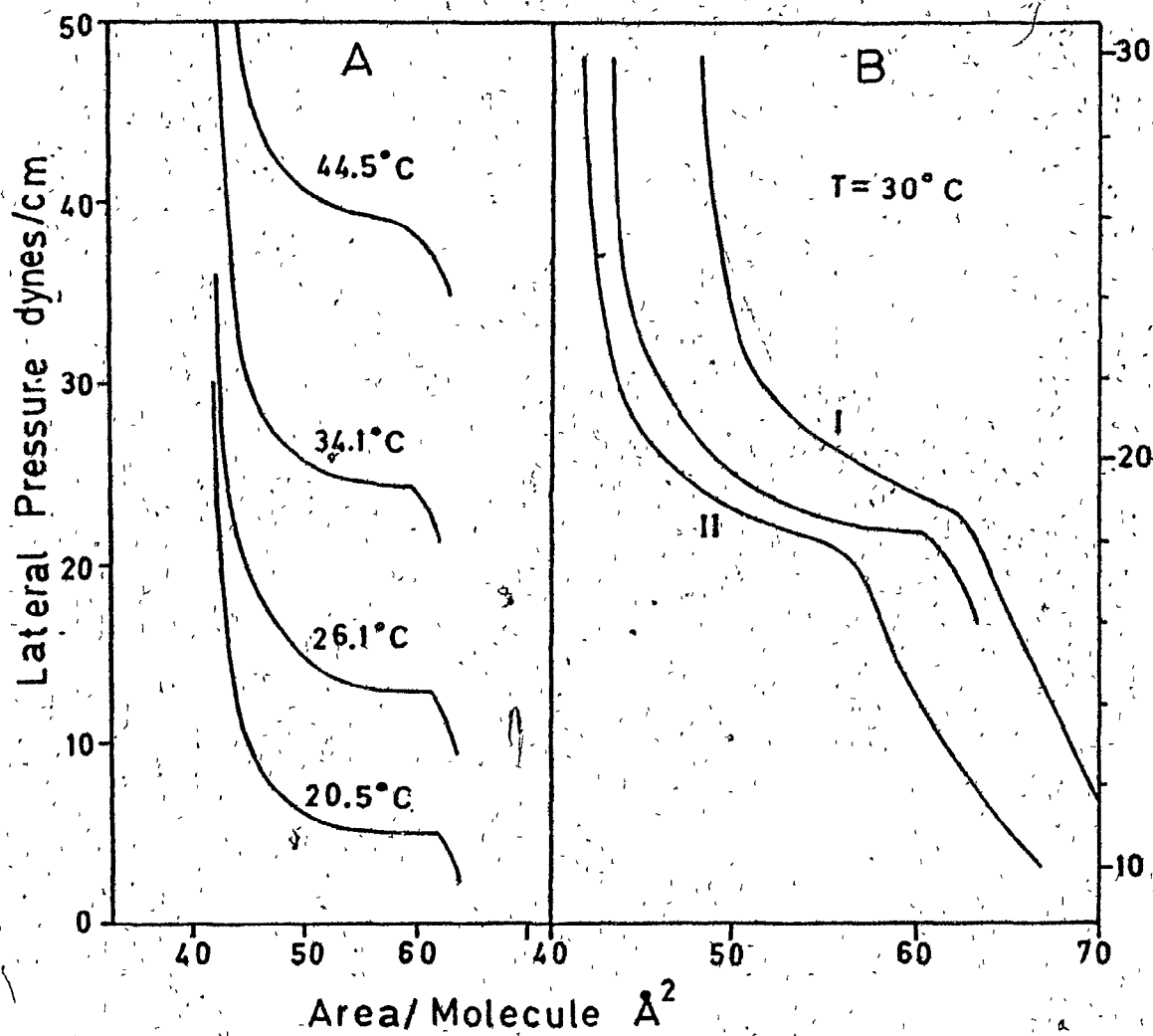


Fig. 2.3 The Cayley tree with $q=3$ and $n=3$ rings. In labelling the lattice we follow the notation of Katsura and Takizawa⁽⁴¹⁾. The vertices are labelled by the indices $0, 1, i_2, \dots, i_1 i_2 \dots i_s$ ($i_1 = 1, 2 \dots q; i_2 i_3 \dots (q-1)$). (taken from A. Georgallas' thesis⁽³¹⁾).

Fig. 2.4 (a) Calculated Π -A isotherms.
(b) Predicted Π -A isotherms for $T=30^\circ\text{C}$ compared
with those obtained by Albrecht et al⁽¹²⁾ (I),
and those obtained by von Tscharner and McConnell
(II)⁽⁴²⁾. (Taken from GP⁽²²⁾).



CHAPTER THREE : THE LIQUID-EXPANDED TO SURFACE-GAS (LE/SG) TRANSITION

This chapter presents a model for the LE/SG phase transition of lipid monolayers based on a two-dimensional lattice gas theory and a change in the orientation of the hydrocarbon chains with respect to the aqueous substrate. We begin by reviewing some experimental data for the LE/SG transition. We continue by presenting our lattice model and end the chapter with a presentation of our model for the complete II - A isotherms of the lipid monolayer.

(1) EXPERIMENTAL RESULTS

Experimentally the LE/SG phase transition is a first-order phase transition. It is characterized by the large range of its coexistence region, which runs from about one hundred to several thousands of angstroms squared. It is found at very low pressures of about 0.12 dynes/cm for pentadecanoic acid to 0.01 dynes/cm for dimyristoyl lecithin, both at $T \sim 25^{\circ}\text{C}$. Kim and Cannell⁽¹⁶⁾, with better experimental techniques, were able to improve upon initial measurements done by Hawkins and Benedek⁽¹⁷⁾. The density of the liquid phase, ρ_l , and the vapour phase, ρ_v , were obtained by fitting the Π data with a polynomial in ρ near each side of the coexistence curve. The intersection of these fitted curves with Π in the horizontal portion of each isotherm leads to the following set of critical exponents :

$$(\kappa)_v = 2.73 \times 10^3 (T_c - T)^{-0.97 \pm 0.004} \text{ cm./dynes}$$

$$(K)_1 = 1.25 \times 10^3 (T_c - T)^{-0.98 \pm 0.007} \text{ cm./dynes}$$

$$(\rho_1 + \rho_v) = 41.9 (T_c - T)^{0.50 \pm 0.003} \text{ mol./ } 10^4 \text{ A}^2$$

[3.1]

$$\rho_c = 41.7 \text{ mol./ } 10^4 \text{ A}^2$$

$$T_c = 26.27^\circ \text{C}$$

$$\Pi_c = 174 \text{ mdynes/cm.}$$

These results are reminiscent of those obtained from mean field calculations, which are known to be exact for infinite range weak interactive forces⁽³³⁾.

There exists some uncertainty as to the exact value of the critical temperature, which may be due to experimental methods. Thus, Kim et al.⁽¹⁶⁾, using a teflon tray found $T_c = 26.27^\circ \text{ C}$. Pallas⁽¹⁵⁾ worked with a fused silica tray estimated the critical temperature to be between 39.4°C to 51.04°C . The difference could be due to the extrusion of surface-active contaminants from the teflon tray.

(ii) LATTICE GAS MODELS

As a gaseous monolayer is compressed, its Π -A isotherms increasingly start to deviate from those of a two-dimensional ideal gas (eq. 1.1). One of the simplest equations of state, which when combined with Maxwell's equal area construction, yields a first-order phase transition in two-dimensions is the van der Waals equation :

$$[3.2] \quad (\Pi + a/A^2)(A - A_0) = kT$$

where a is a cohesive term and A_0 an excluded area term. These are usually adjustable or "fitting" parameters of the theory although Smith⁽³⁴⁾ provides some measure of theoretical justification for their values. The critical point is predicted to be :

$$[3.3] \quad \Pi_c = \frac{a}{27A^2} \quad A_c = 3A_0 \quad T_c = \frac{8a}{27kA_0}$$

The critical exponents have mean-field values⁽³⁵⁾. Both Pallas⁽¹⁵⁾ and Gershfeld⁽³⁶⁾ obtained values for the critical point from their data.

Taking $A_0 = 400 \text{ \AA}^2/\text{mol.}$ and $a = 2.8 \times 10^{-13} \text{ erg.cm.}^2 \text{ mol.}^{-1}$ yields a critical point of $\Pi_c = 929 \mu\text{Nm}^{-1}$, $A_c = 300 \text{ \AA}^2/\text{mol.}$ and $T_c = 266^\circ\text{C.}$

These values are clearly not reasonable. Thus, the van der Waals equation of state fails to provide realistic information about the critical behavior of the LE/SG phase transition of the monolayer. Furthermore, the isotherms generated by this equation of state compare unfavourably to the experimentally obtained isotherms, particularly in regions of high densities.

A first attempt to model the LE/SG phase transition makes use of a simple lattice gas model. It is based on the idea that it is the addition of vacancies which provide the only mechanism for increasing area in the LE phase. The results of such a model are well known.

Hill⁽³⁷⁾ gives the equation of state as :

$$[3-4] \quad \frac{\Pi}{kT} = \ln \left[\frac{[(\beta+1)(1-f)^2]}{(\beta+1-2f)} \frac{q}{(1-f)} \right]$$

$$\beta = [1 + 4(1 - f)(1 - \exp(-E/kT))]^{1/4}$$

where f is the fraction of occupied sites, E is the interaction energy between occupied sites and q denotes the number of nearest neighbours of a site on the lattice ($q = 6$ for triangular lattice). The critical temperature is predicted to be :

$$[3-5] \quad \frac{qE}{kT_c} = 2q \ln \left(\frac{q-2}{q} \right)$$

Selecting $T_c = 31.5^\circ\text{C}$ in accordance with Gershfeld's¹³ results fixes the interaction energy E at $\sim 0.17 \times 10^{-13}$ ergs.. Working on a triangular lattice, we chose the area per site to be 34.0 \AA^2 in accordance with results from the LC/LE phase transition. We then obtained, after Maxwell construction, a first-order phase transition with isotherms akin to those predicted by a van der Waals gas. The coexistence region had a very much smaller range ($\sim 500 \text{ \AA}^2$) than those experimentally observed. This decreased length may be an artifact of the Bethe approximation. However, if we combine the results of this lattice gas model with those of the LC/LE phase transition (as explained in section (iv) of this chapter), the resultant isotherms exhibit very steep slopes in the LE phase. As a result this simple lattice gas model is unsatisfactory as a model for the LE phase. This points to the

existence of a mechanism which is different than the strict addition of vacancies or free volume.

(iii) LATTICE GAS MODEL WITH CHAIN COLLAPSE

The key idea of our model for the LE phase is that the acyl chains of most of the phospholipids lie horizontally on the aqueous substrate in the SG phase and perpendicularly to the interface in the LC phase. This suggests a lifting up of the chains as the film is compressed. We shall not address the question of the motion between these two configurations, but rather regard them as two distinct states of the hydrocarbon chains. At all times the head-group stays well anchored below the aqueous substrate (see fig.(1.3)).

In this model, we start with a triangular lattice of N_s sites. We place upon it N_g straight, rigid and interacting rods, each occupying $(m+1)$ lattice sites. These will represent the lipid molecules with fallen hydrocarbon chains. In addition N_e molecules with upright acyl chains, each taking up one site, are placed on the lattice. Thus, we have essentially a two-state model in terms of chain orientation. The upright chains may be in either their ground state (g) or their excited state (e). Finally we have N_o vacancies or holes. Letting N represent the number of lipid chains, we have :

[3-5]

$$N = N_g + N_e$$

[3-6]

$$N = N_{\uparrow} + N_{\downarrow}$$

[3-7]

$$N_s = N_o + N_e + (m+1)N_g$$

Furthermore, there exist three base vectors on the triangular lattice in whose direction the rigid rods can lie. If N_i denotes the number of rods lying in the i th direction, then :

$$[3-8] \quad N_{\downarrow} = \sum_{i=1}^{\mu} N_i$$

with $\nu = 3$ for our triangular lattice.

The isothermal-isobaric partition function for the monolayer in the LE phase may then be written⁽¹⁰⁾ :

$$[3-9] \quad Z(N_s, N, \Pi, T) = \sum_{N_\alpha} \sum_{N_{\alpha\beta}} \Omega(N_s, N_\alpha, N_{\alpha\beta}) \left[\prod_{\alpha} z_{\alpha}^{N_{\alpha}} \right] \exp[-\mathcal{H}_{LS}/kT]$$

where Ω is the total number of intermolecular configurations for a given value of nearest neighbour $N_{\alpha\beta}$ of type $\alpha\beta$ where $\alpha, \beta \in \{o, e, g, i=1, 2, 3\}$.

The partition function for the α state is of the form :

[3-10]

$$z_{\alpha} = \exp[-f_{\alpha}/kT]$$

with f_{α} denotes the activation energy of the α th state of the lipid chain. We proceed to calculate the unknown elements of the partition function (3-9).

The partition function will be calculated in the quasi-chemical

approximation, which takes first neighbour correlations into account.

Hill shows that⁽³⁷⁾ :

$$[3-11] \quad \sum_{N_{\alpha\beta}} \Omega(N_s, N_\alpha; N_{\alpha\beta}) = g(N_s, N_\alpha)$$

where $g(N_s, N_\alpha)$ represents the number of configurations irrespective of neighbouring arrangements. It is equivalent to the number of ways of laying down N_j rods, N_\uparrow upright molecules and N_0 vacancies on the lattice. Our calculation of $g(N_s, N_\alpha)$ proceeds through a straightforward extension of analysis of DiMarzio⁽³⁸⁾.

We begin with a triangular lattice for which eqs.(3-6) to (3-9) hold. Onto this empty lattice we first place N_g and N_e upright molecules. This may be done in :

$$[3-12] \quad \frac{(N_s)!}{(N_s - N_g)! (N_g)!} \cdot \frac{(N_s - N_g)!}{(N_s - N_g - N_e)! (N_e)!} = \frac{N_s!}{(N_s - N_\uparrow)! (N_g)! (N_e)!}$$

different ways.

We then place j_1 molecules in the first direction onto the lattice. The probability that a site A, picked at random, is empty is :

$$[3-13] \quad P[A \text{ empty}] = \frac{(N_s - N_\uparrow - (m+1)j_1)!}{N_s!}$$

The probability that a site is occupied by a rod segment is :

$$[3-14] \quad P[\downarrow] = \frac{(m+1)j_1}{N_s}$$

If site A is empty, the ratio of the number of times it adjoins a rod to the number of times it adjoins a vacant site is :

$$[3-15] \quad \frac{\left[\frac{1}{(m+1)} \frac{j_1}{N_s} \right]}{\left[\frac{(N_s - N_{\uparrow} - (m+1)j_1)}{N_s} \right]} = \frac{j_1}{(N_s - N_{\uparrow} - (m+1)j_1)}$$

The probability that a site B is empty, given that it adjoins an empty site A is :

$$[3-16] \quad P[A, B \text{ empty}] = \frac{(N_s - N_{\uparrow} - (m+1)j_1)}{(N_s - N_{\uparrow} - (m+1)j_1) + j_1}$$

The $(j_1 + 1)$ molecule may then be placed onto the lattice in μ_{j+1} ways:

$$[3-17] \quad \mu_{j+1} = \left[\frac{(N_s - N_{\uparrow} - (m+1)j_1)}{(N_s - N_{\uparrow} - m j_1)} \right]^m (N_s - N_{\uparrow} - (m+1)j_1)$$

The total number of ways to place N_1 indistinguishable molecules onto the lattice in the first orientation is :

$$[3-18] \quad \prod_{i=0}^{M-1} \frac{\mu_{j_1 + i}}{N_1!} = \frac{[N_s - N_{\uparrow} - (m+1)N_1 + N_1]! [N_s - N_{\uparrow}]!}{[N_s - N_{\uparrow}]! [N_1!] [N_s - N_{\uparrow} - (m+1)N_1]!}$$

$$= \frac{[N_s - N_{\uparrow} - mN_1]!}{N_1! [N_s - N_{\uparrow} - (m+1)N_1]!}$$

Given that N_1 molecules have been placed in direction 1, we proceed to add N_2 molecules in direction 2, assuming that each direction is independent of the other. We again first add j_2 molecules.

The $(j_2 + 1)$ th molecule can then go onto the lattice in $(N_s - N_{\uparrow} - (m+1)N_1 - (m+1)j_2)$ places. The probability that a site is unoccupied when it is known that the adjacent site in the second direction is occupied is :

$$[3-19] \quad P[A, B \text{ empty}] = \frac{[N_s - N_{\uparrow} - (m+1)N_1 - (m+1)j_2]}{[N_s - (m+1)(N_1 + j_2) - N_{\uparrow} + (m+1)N_1 + j_2]}$$

It follows that :

$$[3-20] \quad \mu_{j_2+1} = \left[\frac{[N_s - N_{\uparrow} - (m+1)(N_1 + j_2)]}{[N_s - (m+1)(N_1 + j_2) + (m+1)N_1 + j_2 - N_{\uparrow}]} \right]^m [N_s - N_{\uparrow} - (m+1)(N_1 + j_2)]$$

We have :

$$[3-21] \quad \prod_{k=0}^{N_2-1} \frac{\mu_{j_2+1}}{N_2!} = \frac{[N_s - N_{\uparrow} - (m+1)N_1]! [N_s - N_{\uparrow} - mN_2]!}{N_2! [N_s - N_{\uparrow}]! [N_s - N_{\uparrow} - (m+1)(N_1 + N_2)]!}$$

Proceeding in the same way for the third direction :

$$[3-22] \quad \mu_{j_3+1} = \left[\frac{[N_s - N_{\uparrow} - (m+1)(N_1 + N_2 + j_3)]}{[N_s - N_{\uparrow} - (m+1)(N_1 + N_2 + j_3) + (m+1)(N_1 + N_2) + j_3]} \right]^m [N_s - N_{\uparrow} - (m+1)(N_1 + N_2 + j_3)]$$

$$[3-23] \quad \prod_{j_3=0}^{N_3-1} \frac{\mu_{j_3+1}}{N_3!} = \frac{[N_s - N_{\uparrow} - (m+1)(N_1 + N_2)]! [N_s - N_{\uparrow} - mN_3]!}{N_3! [N_s - N_{\uparrow}]! [N_s - N_{\uparrow} - (m+1)(N_1 + N_2 + N_3)]!}$$

Multiplication of eqs.(3-12,17,20,23) yields the $g(N_s, N_{\alpha})$ factor for N_s rods, N_{\uparrow} upright molecules and N_o vacancies :

$$[3-24] \quad g(N_s, N_\alpha) = \frac{N_s! \prod_{j=1}^M [N_s - N_\alpha - mN_j]!}{[N_s - N_\alpha]!^3 N_o! N_g! N_e! \prod_{j=1}^M [N_j]!}$$

If the distribution of rods over the possible lattice directions is isotropic - i.e. $N_j = N_s/3$:

$$[3-25] \quad g(N_s, N_\uparrow, N_\downarrow, N_o) = \frac{N_s! [N_s - N_\uparrow - \frac{m}{3}N_\downarrow]!^3}{[N_s - N_\uparrow]!^3 N_o! N_g! N_e! [\frac{N_\downarrow}{3}]!^3}$$

In the special case of $N_\uparrow = 0$, this reduces to :

$$[3-26] \quad g(N_s, N_\downarrow, N_o) = \frac{[N_s - \frac{m}{3}N_\downarrow]!^3}{N_s!^2 N_o! [\frac{N_\downarrow}{3}]!^3}$$

which is the formula published by DiMazio (38).

Finally taking the logarithm of eq.(3-25), applying Stirling's approximation and eliminating N_α for convenience :

$$\begin{aligned} \ln(g)/N &= (1+y_\uparrow + my_\downarrow) \ln(1+y_\uparrow + my_\downarrow) + y_\uparrow \ln(y_\uparrow) + y_\downarrow \ln(y_\downarrow/\mu) \\ &\quad + \mu(y_\uparrow + (\frac{\mu+1}{\mu}m+1)y_\downarrow) \ln(y_\uparrow + (\frac{\mu+1}{\mu}m+1)y_\downarrow) - y_\downarrow \ln(y_\downarrow) \\ [3-27] \quad &\quad -(1-y_\uparrow - y_\downarrow) \ln(1-y_\uparrow - y_\downarrow) - \mu(y_\uparrow + (m+1)y_\downarrow) \ln(y_\uparrow + (m+1)y_\downarrow) \end{aligned}$$

where $\nu = 3$ for a triangular lattice and $y_\alpha = N_\alpha/N_s$.

In the partition function (3-10) we have the following Hamiltonian:

$$[3-28] \quad \mathcal{H}_{LS} = \sum_{\alpha, \beta} N_{\alpha\beta} \epsilon_{\alpha\beta} + \Pi A_t$$

where $N_{\alpha\beta}$ represents the number of nearest neighbours of type $\alpha\beta$ with $\alpha, \beta \in \{e, g, l\}$; $e_{\alpha\beta}$ represents the yet unspecified interaction energy between molecules of type α and β ; Π represents the surface pressure and A_t the total area of the monolayer:

$$A_t = A_e N_{eo} + A_g N_{gg} + A_e N_{ee} + A_e (m+1) N_{el}$$

[3-29]

$$= N_e [A_e (y_0 + (m+1)y_1 + 1 - y_2 - y_3) + A_g y_1]$$

Here A_e , the area occupied by an upright, melted chain is taken to be the area of a vacancy; fallen chains are assumed to occupy an area proportional to A_e .

If the set $\{N_{\alpha\beta}\}$ were known, we would then be in a position to calculate all the elements of the partition function. This set will now be calculated in the quasi-chemical approximation through an extension of work by Cotter-Martire⁽³⁹⁾.

Working with our familiar triangular lattice, we again assume that rods lying in the three different directions to be formally different species. We then have 36 different types of nearest neighbour configurations subject to the constraints:

[3-30]

$$2N_{\alpha\alpha} + \sum_{\beta \neq \alpha} (N_{\alpha\beta} + N_{\beta\alpha}) = q_\alpha z N_\alpha$$

where ($q_0 = q_e = q_g = 1, q_1 = ((m+1)z - 2(m+1) + 2)$) with $z=6$. Here q_z represents the number of nearest neighbours a molecule of type α has. In our calculations, we will choose $\{N_{\alpha\beta} / \alpha\beta \in \{o, e, g, i=1, 2, 3\}\}$ as the

- 30 -

set of independent variables and determine $\{N_{\alpha\alpha}\}$ using the above equations of constraint.

In the quasi-chemical approximation, which is equivalent to the Bethe approximation in two-dimensions, we treat neighbouring sites as independent. A combinatorial approach will then be used to calculate $\omega(N_s, N_{\alpha\beta})$, the number of ways of randomly arranging $N_{\alpha\beta}$ pairs assuming complete independence for all pairs.

[3-31]

$$g(N_s, N_\alpha; N_{\alpha\beta}) = C(N_\alpha) \omega(N_s, N_\alpha; N_{\alpha\beta})$$

We expect $C \ll 1$, since many physically impossible situations will be counted in ω . From combinatorics :

[3-32]

$$\omega = \frac{\sum_{\alpha, \beta} (N_{\alpha\alpha} + N_{\alpha\beta} + N_{\beta\alpha})!}{\prod_{\alpha} N_{\alpha\alpha}! \prod_{\alpha, \beta} (N_{\alpha\beta}! N_{\beta\alpha}!)!} ; \alpha \neq \beta$$

Utilizing the equations of constraint, this becomes :

[3-33]

$$\omega = \frac{\sum_{\alpha} q_\alpha N_\alpha}{\prod_{\alpha} (q_\alpha z N_\alpha - \sum_{\beta} (N_{\alpha\beta} + N_{\beta\alpha})!) \prod_{\alpha, \beta} (N_{\alpha\beta}! N_{\beta\alpha}!)!} ; \alpha \neq \beta$$

To obtain C , we sum over $N_{\alpha\beta}$:

[3-34]

$$g(N_s, N_\alpha) = C(N_\alpha) \sum_{N_{\alpha\beta}} \omega(N_s, N_\alpha; N_{\alpha\beta})$$

Since the value of $g(N_s, N_\alpha)$ is given by eq.(3-25), we can, in principle, now determine $C(N_\alpha)$. However, the sum is much too difficult to perform directly. We therefore make use of the "maximum term method", which

replaces the logarithm of a sum by the logarithm of the largest term in the sum. Hill shows that to orders of magnitude significant in thermodynamics, the two are equal⁽³⁷⁾. Therefore :

$$[3-35] \quad \ln(C) = \ln(g(N_s, N_\alpha)) - \ln(\omega_{\max.})$$

It turns out to be more convenient to maximize $\log \omega$:

$$\begin{aligned} \ln \omega &= \frac{z}{2} \left[\sum_\alpha q_\alpha N_\alpha \right] \ln \left[\sum_\alpha \frac{z}{2} q_\alpha N_\alpha \right] \\ &\quad - \frac{z}{2} \left[z q_\alpha N_\alpha - \sum_{\beta \neq \alpha} (N_{\alpha\beta} + N_{\beta\alpha}) \right] \ln \left[\frac{z}{2} (q_\alpha z N_\alpha - \sum_{\beta \neq \alpha} (N_{\alpha\beta} + N_{\beta\alpha})) \right] \\ [3-36] \quad &\quad - \sum_{\alpha \neq \beta} [N_{\alpha\beta} \ln(N_{\alpha\beta}) + N_{\beta\alpha} \ln(N_{\beta\alpha})] \end{aligned}$$

Maximizing this w.r.t. the set $N_{\alpha\beta}$ and $N_{\beta\alpha}$ yields the set of simultaneous equations :

$$[3-37] \quad \frac{4N_{\alpha\beta}^2}{[\sum_\gamma (q_\alpha z N_\alpha - (N_{\alpha\gamma} + N_{\gamma\alpha}))][\sum_\gamma (q_\beta z N_\beta - (N_{\beta\gamma} + N_{\gamma\beta}))]} = 1$$

$\alpha, \beta \in \{o, g, e, i=1, 2, 3\}$

These may be solved to give :

$$\begin{aligned} N_{\alpha\beta} = N_{\beta\alpha} &= \frac{q_\alpha q_\beta z N_\alpha N_\beta}{2 [\sum_\gamma q_\gamma N_\gamma]} \\ [3-38] \quad &= \frac{q_\alpha q_\beta z y_\alpha y_\beta N}{2(1 + y_o + (q-1)y_i)} \\ &\quad \gamma \in \{o, g, e, i=1, 2, 3\} \end{aligned}$$

We now have all the ingredients necessary to calculate the partition function. The Gibbs free energy may now be written down using

eqs.(3-27), (3-28), (3-29), (3-38) :

$$G/N = -kT \ln(Z)/N$$

$$\begin{aligned}
 &= -kT \left\{ (1+y_0 + my_\downarrow) \ln(1+y_0 + my_\downarrow) - y_0 \ln(y_0) \right. \\
 &\quad - (1-y_\downarrow - y_g) \ln(1-y_\downarrow - y_g) - y_g \ln(y_g) - y_\downarrow \ln(\frac{y_\downarrow}{\mu}) \\
 &\quad + \mu(y_0 + (\frac{\mu-1}{\mu}m+1)y_\downarrow) \ln(y_0 + (\frac{\mu-1}{\mu}m+1)y_\downarrow) \\
 &\quad \left. + \mu(y_0 + (m+1)y_\downarrow) \ln(y_0 + (m+1)y_\downarrow) \right\} \\
 &+ \frac{z}{2(1+y_0 + (q-1)y_\downarrow)} \left\{ y_g \epsilon_{gg} + 2y_g (1-y_\downarrow - y_g) \epsilon_{eg} + 2qy_g y_\downarrow \epsilon_{g\downarrow} \right. \\
 &\quad \left. + (1-y_g - y_\downarrow)^2 \epsilon_{ee} + 2q(1-y_\downarrow - y_g) y_\downarrow \epsilon_{e\downarrow} + q^2 y_\downarrow^2 \epsilon_{\downarrow\downarrow} \right\} \\
 [3-39] \quad &+ \Pi(A_e my_\downarrow + A_e y_0 + (A_g - A_e)y_g + A_e) + f_\downarrow y_\downarrow
 \end{aligned}$$

We have assumed that vacancies do not interact with any other particle

i.e. $\epsilon_{\alpha\alpha} = 0$. Minimizing the Gibbs free energy w.r.t. y_0 and y_\downarrow ,

subject to the constraint that N is constant yields the set of coupled equations :

$$\begin{aligned}
 &kT \left\{ m \ln[1-y_0 - my_\downarrow] + \mu(\frac{\mu-1}{\mu}m+1) \ln[y_0 + (\frac{\mu-1}{\mu}m+1)y_\downarrow] \right. \\
 &\quad \left. - \ln[\frac{y_\downarrow}{\mu}] + \ln[1-y_\downarrow - y_g] + \mu(m+1) \ln[y_0 + (m+1)y_\downarrow] \right\} \\
 &+ \frac{z}{2(1+y_0 + (q-1)y_\downarrow)} \left\{ 2(1-y_\downarrow - y_g) \epsilon_{ee} - 2qy_g \epsilon_{g\downarrow} \right. \\
 &\quad \left. - 2q(1-2y_\downarrow - y_g) \epsilon_{e\downarrow} + 2y_g \epsilon_{eg} - 2q^2 y_\downarrow \epsilon_{\downarrow\downarrow} \right\} \\
 &+ \frac{z(q-1)}{2(1+y_0 + (q-1)y_\downarrow)} \left\{ y_g \epsilon_{gg} + (1-y_g - y_\downarrow)^2 \epsilon_{ee} \right. \\
 &\quad \left. + 2(1-y_g - y_\downarrow) y_g \epsilon_{eg} + 2q(1-y_g - y_\downarrow) y_\downarrow \epsilon_{e\downarrow} + 2qy_g y_\downarrow \epsilon_{g\downarrow} + q^2 y_\downarrow^2 \epsilon_{\downarrow\downarrow} \right\} \\
 [3-40] \quad &= f_\downarrow + m A_e \Pi
 \end{aligned}$$

$$\begin{aligned}
 & kT \left\{ \ln[1+y_0 + my_1] - \ln[y_0] + \mu \ln[y_0 + (\frac{\mu-1}{\mu}m+1)y_1] \right. \\
 & \quad \left. - \ln[y_0 + (m+1)y_1] \right\} \\
 & + \frac{z}{2(1+y_0 + (q-1)y_1)^2} \left\{ y_g \epsilon_{gg} + (1-y_g - y_1)^2 \epsilon_{ee} \right. \\
 & \quad \left. + 2(1-y_g - y_1)y_g \epsilon_{eg} + q^2 y_1^2 \epsilon_{ll} + 2q(1-y_g - y_1)y_1 \epsilon_{el} + 2qy_g y_1 \epsilon_{gl} \right\} \\
 [3-41] \quad & = \frac{\Pi_A}{g}
 \end{aligned}$$

The above equations may be solved numerically to yield the II - A isotherms for the LE/SG phase transition.

(iv) A MODEL FOR THE COMPLETE II - A ISOTHERMS

Up to now we have dealt with the LC/LE and LE/SG transition separately. The Hamiltonian which will generate the complete II - A isotherms of the lipid monolayer may be written :

$$[3-42] \quad \mathcal{H} = \mathcal{H}_{GP} + \mathcal{H}_{LS} + \mathcal{H}_{coupling}$$

where \mathcal{H}_{GP} represents the Hamiltonian developed by Georgallas and Pink^(22,27) for the LC/LE transition ; \mathcal{H}_{LS} is the Hamiltonian for the LE/SG transition and $\mathcal{H}_{coupling}$ the coupling Hamiltonian which will connect the two phases. Since the \mathcal{H}_{GP} and \mathcal{H}_{LS} generate phase transitions that are effectively separated, we will suppose that

$\mathcal{H}_{coupling}$ is small and hence makes only a negligible contribution to the system. We can therefore just add free energy contributions from the models developed for the two phase transitions.

Up to now, the interaction energies $\{ \epsilon_{\alpha\beta} \}$ are entirely featureless. It is essential that the values chosen reflect the physical origin of the forces involved. We shall adopt the view that the principle forces involved are the van der Waal dispersive forces and the dipole-dipole interaction between polar head groups. Therefore, we choose :

$$[3-42] \quad \epsilon_{gg} = J_0 I(g,g) + K_0$$

$$\epsilon_{eg} = J_0 I(e,g) + K_0$$

$$\epsilon_{ee} = J_0 I(e,e) + K_0$$

$$\epsilon_{g\downarrow} = \epsilon_{e\downarrow} = \beta K_0$$

$$\epsilon_{\downarrow\downarrow} = \alpha K_0$$

Here $J_0 I(g,g)$, $J_0 I(e,g)$ and $J_0 I(e,e)$ are identical with the parameters given in chapter II. We further have assumed that there will be a negligible contribution to the van der Waals interaction between chains oriented at right angles to each other. K_0 denotes the contribution from the dipole-dipole interaction. In the case of the interaction between fallen and upright chains, and between two fallen chains, this interaction will be reduced by a factor of β and α respectively. These parameters are expected to have values less than unity, since not all configurations on the lattice allow for maximal interaction between the polar head groups. For example, consider two

molecules with fallen chains. Only when the two polar head groups are nearest neighbours do they interact with their full-scale attractive force K_0 . Given the very large number of vacancies in the system, and the different configurations that the fallen chains can assume on the lattice, we see that such configurations are very unlikely. Thus, in a very simple fashion, these two parameters account for the distance dependence of the dipole-dipole interaction.

Chapter IV : Results for the Complete Model

In this chapter we present the numerical results for the complete model developed in the last chapter. We first discuss the parameters of the theory, and then present the results through a series of graphs.

In order to solve our equations self-consistently, we combined eqs.(3.40,41) through the elimination of Π . The resultant equation was then solved for y_0 , the concentration of holes, and y_f , the concentration of molecules with fallen chains, both normalized with respect to the number of chains. The Maxwell construction was then applied to the resultant isotherms by checking for equal values of the Gibbs free energy.

In our theory for the LE/SG transition, the adjustable parameters are :

m - the number of lattice sites which a fallen chain occupies on the interface.

f_f - the activation energy associated with the fallen state.

K_0, α, β - these three parameters determine the strengths of the dipole-dipole interactions between various species: K_0 the full-scale dipole-dipole interaction energy; α determines the interaction between two fallen chains; β the interaction between a fallen chain and an upright molecule.

Our numerical results are given through a series of graphs (figs.

4.1.8). We chose to model the isotherms of the phospholipid DPPC, using the following set of parameters :

$J(g,g) = 1.0$	$A_g = 20.4 \text{ } \text{\AA}^2$
$J(e,g) = 0.148$	$A_e = 34.0 \text{ } \text{\AA}^2$
$J(e,e) = 0.022$	$D_g = 1.0$
$J_0 = 0.972 \times 10^{-13} \text{ ergs.}$	$D_e = 1275000.0$
$E_g = 0.0$	$N_0 = 10^2$
$E_e = 2.78 \times 10^{-13} \text{ ergs.}$	$N_s = 10^{10}$

These values are identical with those used by GP in their theory for the LC/LE transition. In the following set of diagrams (see p. 49), unless otherwise specified, the values of the various parameters for the extended model are:

$$T = 21.5^\circ\text{C}$$

$$K_0 = 0.75 \times 10^{-13} \text{ ergs.}$$

$$\beta = 0.55$$

$$\alpha = 0.0$$

$$f_l = 0.0$$

$$m = 5$$

The choice of the above parameters will become clear as we begin to study the effect of each variable.

The first graph (4.1) shows the resultant $\Pi \cdot A$ isotherm for a lipid system without any dipole-dipole interactions at all. As expected,

there is no LE/SG phase transition and the isotherms tend to zero at infinite areas per molecule. Since the case $K_0 < 0$ does not yield any phase transition, we continue to investigate cases with an attractive dipole-dipole interaction.

First we investigate the effect of f_{\downarrow} , the activation energy of the fallen state, on both the LE and SG phases (fig.(4.2)). Increasing f_{\downarrow} draws the monolayer closer together in the LE phase and lowers the pressure at which the LE/SG phase transition takes place. Thus, in order to fit our numerical results to those obtained through experiment, it would seem that an $f_{\downarrow} \sim 10^{-13}$ ergs. is needed. However, choosing $f_{\downarrow} > 0$ leads to an increase in the number of upright chains in the SG phase. This is completely unreasonable in the context of our physical model. Since choosing f_{\downarrow} more negative raises the LE/SG transition pressure, we can therefore dispense with the parameter entirely and set $f_{\downarrow} = 0.0$. This is not unreasonable, since it should cost us no energy to collapse the chains if there is sufficient space.

The effect of changing the amount of space which a fallen chain occupies on the isotherms is shown in fig.(4.3). As m increases from 3 to 7, the isotherms move towards extended areas per molecule. The onset of the LE phase is also increased very slightly ($\sim 2.3 \text{ \AA}^2/\text{mol.}$). Larger values of m depress the pressures at which the LE/SG phase transition takes place. Since the length of a single carbon-carbon bond is about 1.54 \AA , and because a site of our lattice has an area of 34.0

Å^2 , we cannot realistically expect m to take on values greater than 5 (for DPPC, which has two 16-carbon atom chains).

The effect of varying K_0 , the full-scale attractive dipole-dipole interaction strength is illustrated in fig.(4.4). As expected, increasing K_0 results in a less expanded monolayer i.e. the film is drawn closer together. The parameters α and β determine the interaction strengths between two lipids with fallen chains and a lipid with fallen chain and a lipid with an upright chain. Graphs showing the variation of these two parameters are found in fig.(4.5,6). From our physical model and based on the distance dependence of the dipole-dipole interaction, we expect that α will be very small and β to be about 1/2. It is clear that increasing α leads to a more expanded monolayer. The parameter β behaves in the same fashion, except that the variation is much more pronounced. It was found that choosing $K_0 = 0.75 \times 10^{-13}$ ergs., $\beta = 0.55$, $\alpha = 0$ lead to a best fit for the LE phase of the lipid monolayer.

The final results of our model calculations are shown in figs.(4.7,8). In the first, we illustrate the LC/LE phase transition and our results for the LE phase. There has been no attempt made to show the LE/SG phase transition on this figure. The results for the LE/SG phase transition and SG phase are given in fig.(4.8) These show the LE/SG transition as taking place at pressures of 0.12 dynes/cm. ($T \sim 25^\circ\text{C}$) with the length of the coexistence curve being $8,000 - 10,000 \text{ Å}^2/\text{mol.}$

Thus, we see that in a qualitative way, our model reproduces all of the essential features of the two main phase changes of lipid monolayers. In particular, the model of Georgallas and Pink yields nonzero slopes in the coexistence region, and a discontinuous change in slope at the onset of the LE phase. Slopes obtained for the LE phase are in good qualitative agreement with those obtained through experiment. In addition, our model produces a first-order LE/SG phase transition with a coexistence region $> 7,000 \text{ \AA}^2$. We have therefore accomplished our goal of describing the II - A isotherms of lipid monolayers and their associated phase transitions using a single model.

Our model cannot predict the critical behavior of the LE/SG phase transition correctly due to the nature of the Bethe approximation used. Our calculated critical temperature is greater than 300° C . Near the critical point, the variation of the order parameter with temperature is almost parabolic, for a mean-field theory. Thus, for mean-field type solutions, small variations in temperature lead to relatively large changes in the order parameter. This is in contrast to the exact solution, where large changes in the order parameter occur only relatively close to the critical temperature⁽⁴⁰⁾. Hence, if we are to model a very large range in area per molecule using a mean-field type solution, we must be very far from the critical point. Our obtaining values for the critical temperature and pressures which are much too high is not too surprising and corresponds to trends observed in other

models. For example, Pallas⁽¹⁵⁾ obtained a value of $T_c = 260^\circ C$ in fitting data of Gershfeld⁽³⁶⁾ to a mean-field van der Waals equation of state. Furthermore, the data used was for pentadecanoic acid, a soap with a single 15 carbon atom chain and a coexistence curve having a length of about half the size of the corresponding two-chained phospholipid. On this basis alone, our predicted values for the critical temperature should be even farther away from their true value.

One problem with our model is that the predicted pressure values for the LE/SG phase transition are too high. It was possible to reach low pressures of ~ 0.02 dynes/cm. (as observed experimentally) as opposed to our calculated values of ~ 0.12 dynes/cm., but only at the cost of expanding the range of the coexistence region to unreasonable lengths (i.e. $>20,000 \text{ \AA}^2 / \text{mol.}$). Alternately, proper transition pressures and areas could be obtained by accepting lower transition temperatures (say $5-10^\circ C$ as opposed to $25^\circ C$ and higher). Since this would not alter our conceptual picture in any way, this possibility was not fully explored. Our lower transition pressures are partially due to our use of the Bethe approximation and to some of the assumptions implicit in our model.

Our model of the LE/SG phase transition is essentially a two-state model in terms of chain orientation with respect to the aqueous substrate. The hydrocarbon chains are in either their 'upright' or 'fallen state'. No attempt has been made in this thesis to address the dynamics

of the collapse. It seems likely that this collapse or lifting up of the acyl chains takes place in stages, each of which would have its own interaction energy and statistics. Inclusion of such intermediate states into our model may well improve quantitative agreement with the experimental results.

Furthermore, in calculating the statistics for configurations of collapsed chains, molecules with upright chains and vacancies on our triangular lattice, we treated each chain as being completely separate and independent. This makes our model really more appropriate for single-chained molecules such as soaps. Indeed, for such systems, the pressures obtained are in good agreement with those obtained through experiment. In the case of phospholipids such as DPPC, there are always two chains per molecule, which are coupled via their glyceride backbone. Thus our calculations for the entropic terms contributing towards the free energy of the system are only a first approximation.

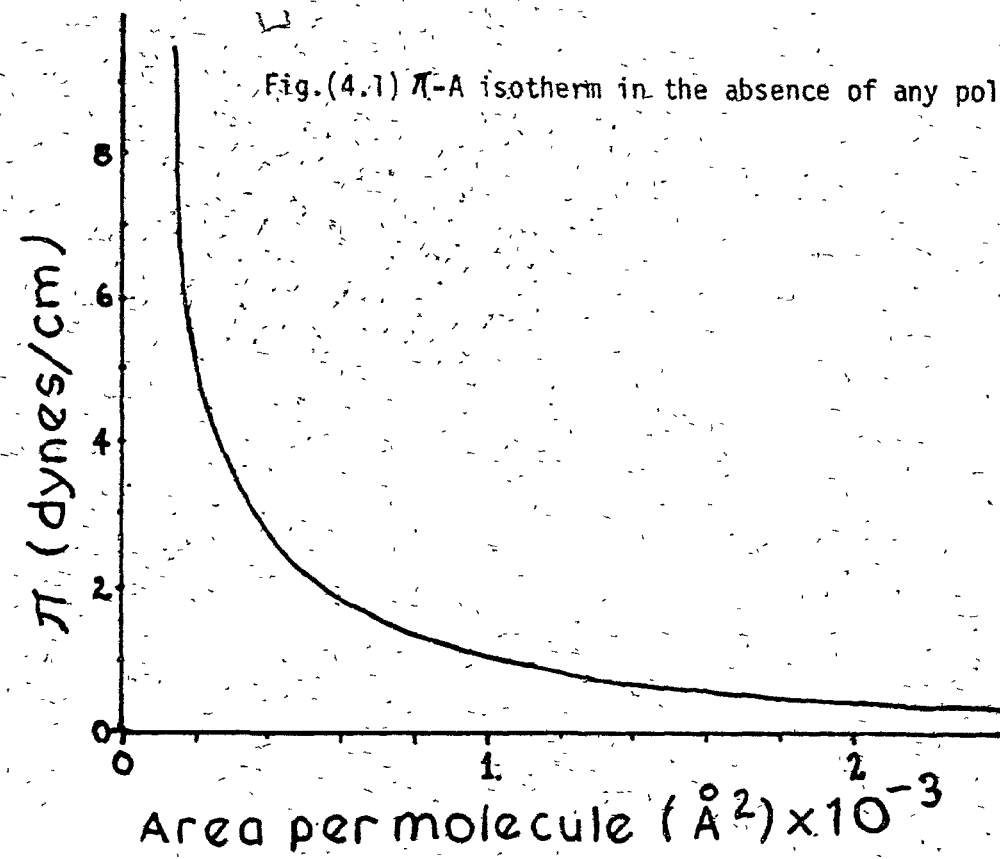


Fig.(4.1) π -A isotherm in the absence of any polar head interaction.

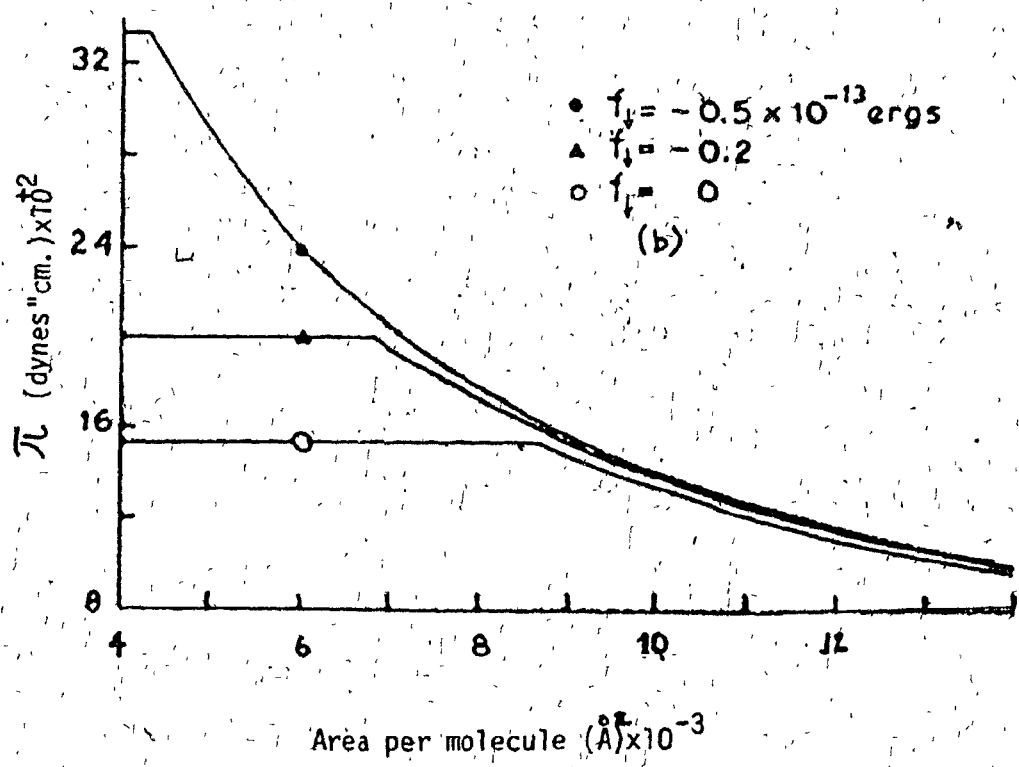
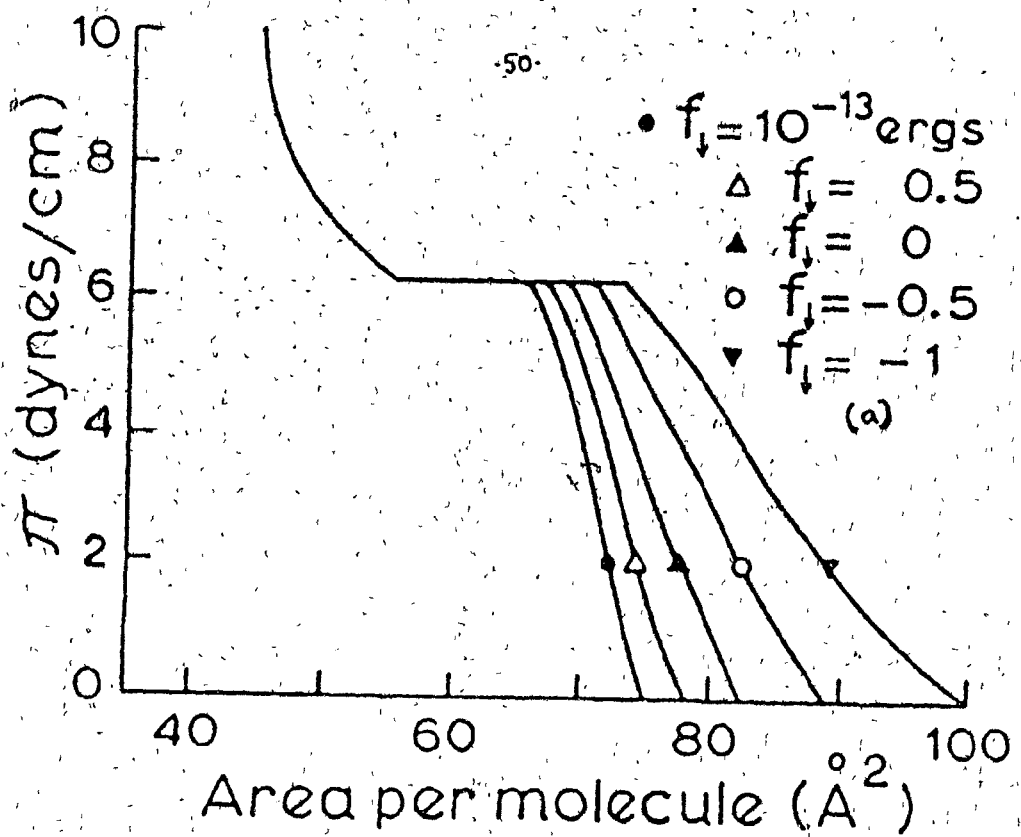


Fig.(4.2) - π -A isotherms showing variation in f_1 , the activation energy of collapsed chain. a) LC/LE transition b) LE/SG transition.

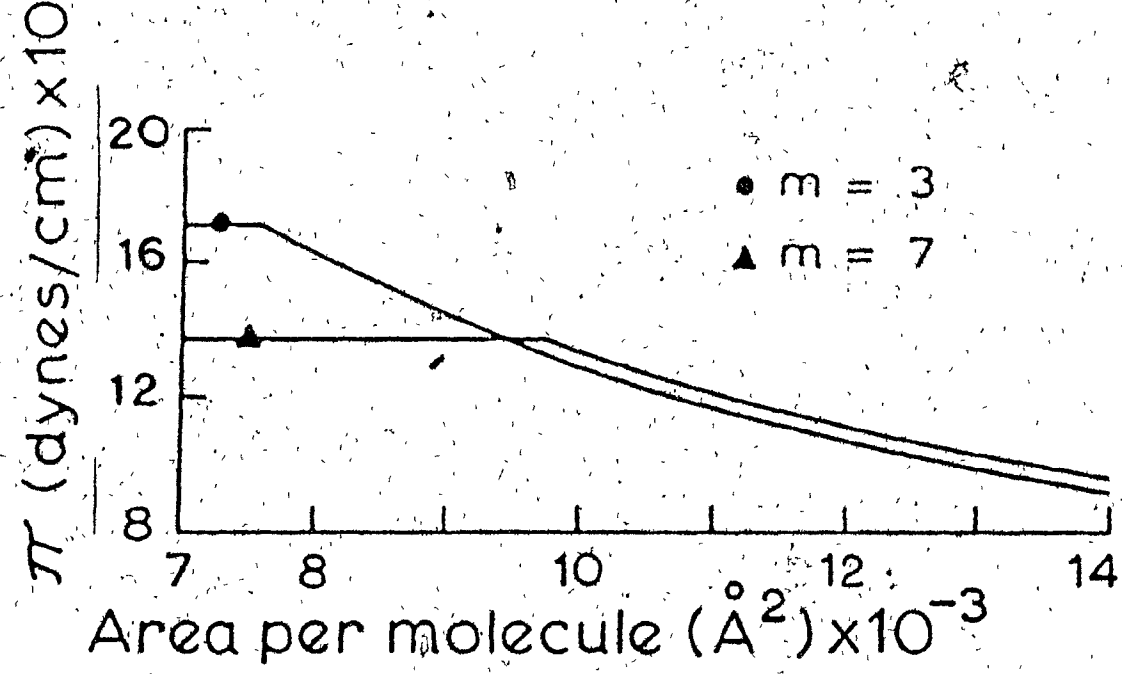
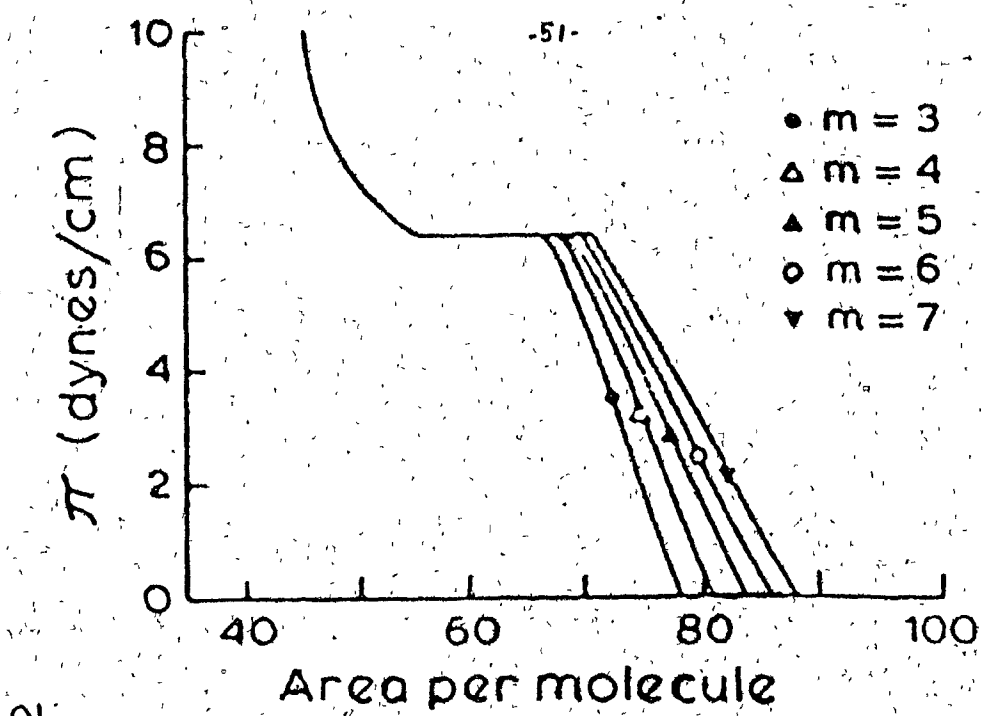


Fig.(4.3)- π -A isotherms showing variation in m , the collapsed chain length . a) LC/LE transition b) LE/SG transition .

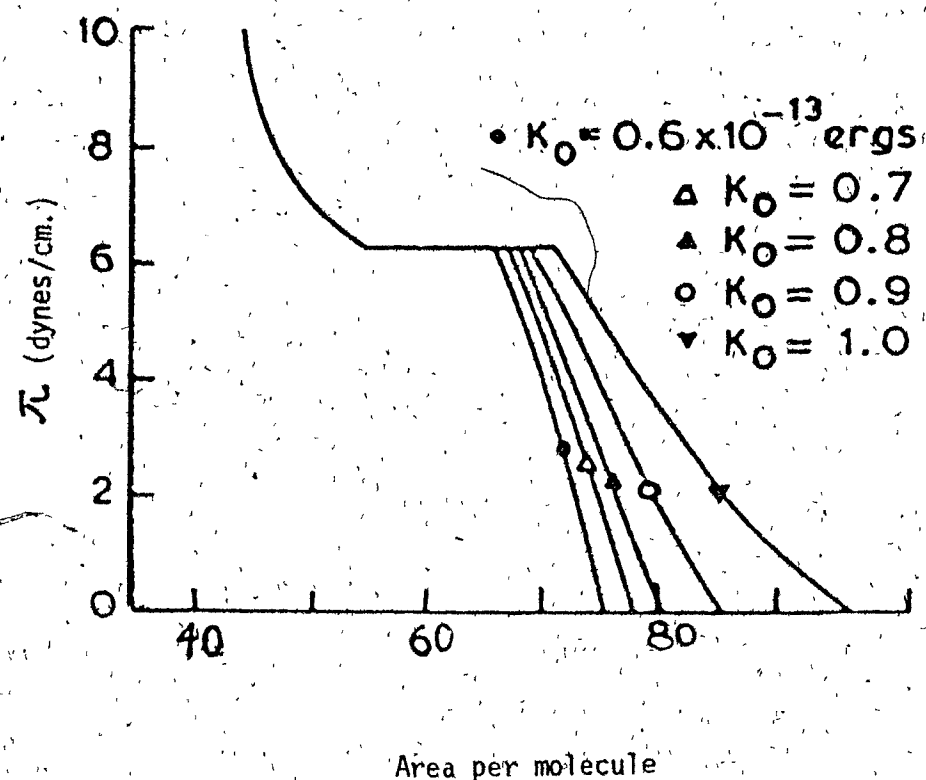


Fig.(4.4) π -A isotherms for the LC/LE transition showing variation of K_0 , the fullscale dipole-dipole interaction.

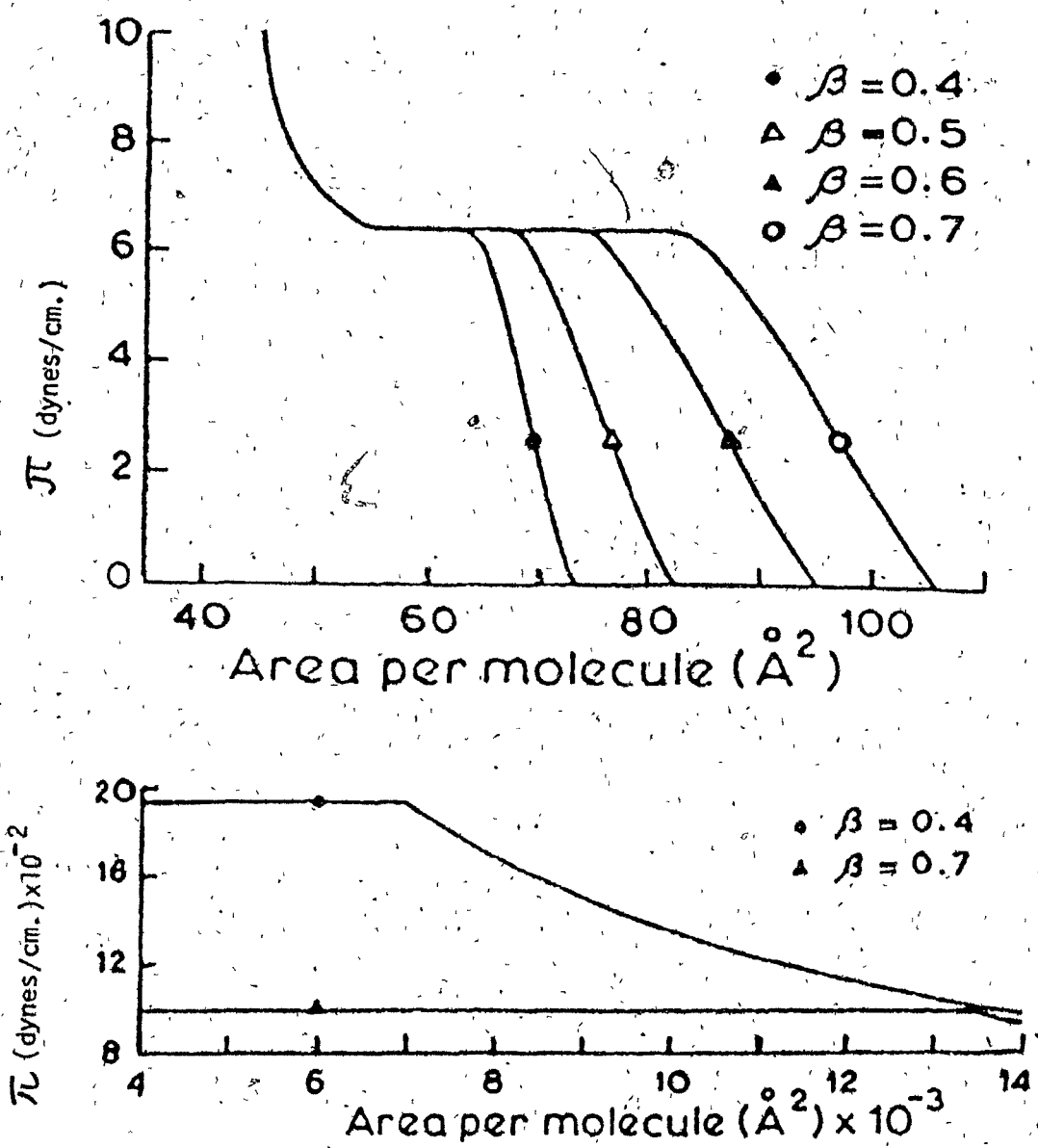


Fig.(4.5) π -A isotherms showing variation of β , the parameter controlling the interaction between a collapsed and upright chain.
 a) LC/LE phase transition. b) LE/SG transition.

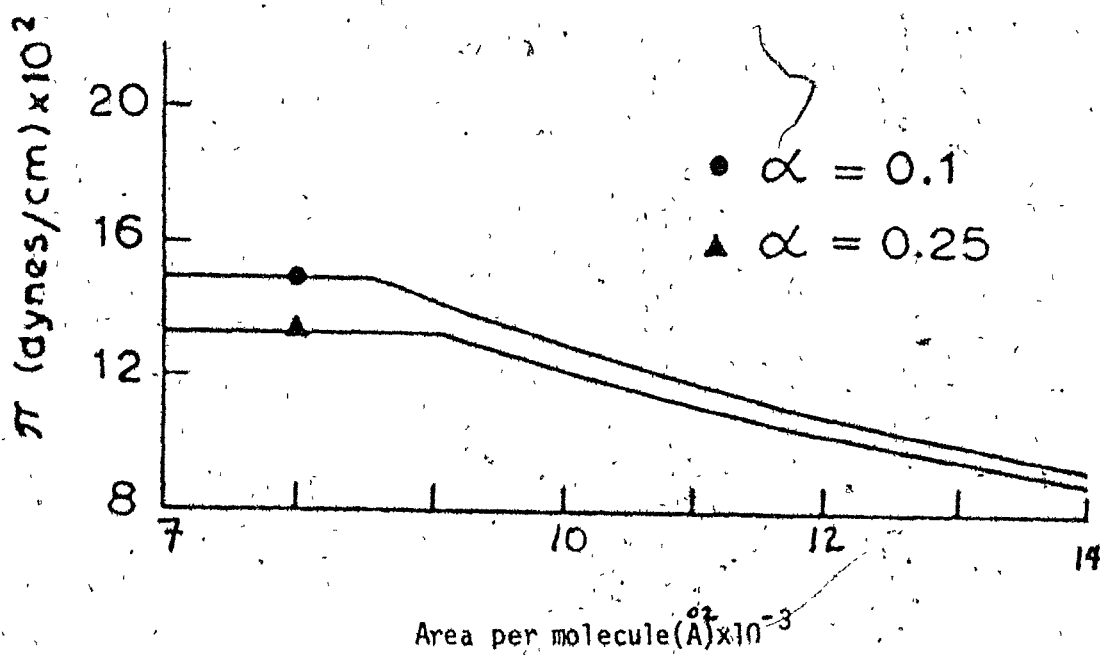
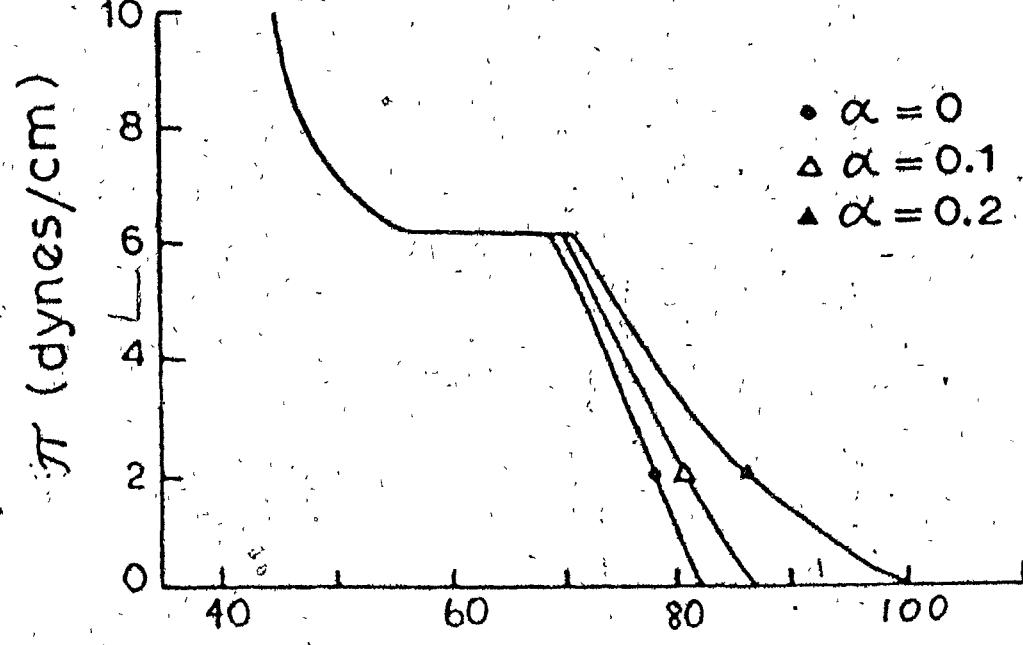


Fig.(4.6) π -A isotherms illustrating change with respect to α , the parameter controlling the dipole interaction between collapsed chains. a) LC/LE phase transition b) LE/SG transition.

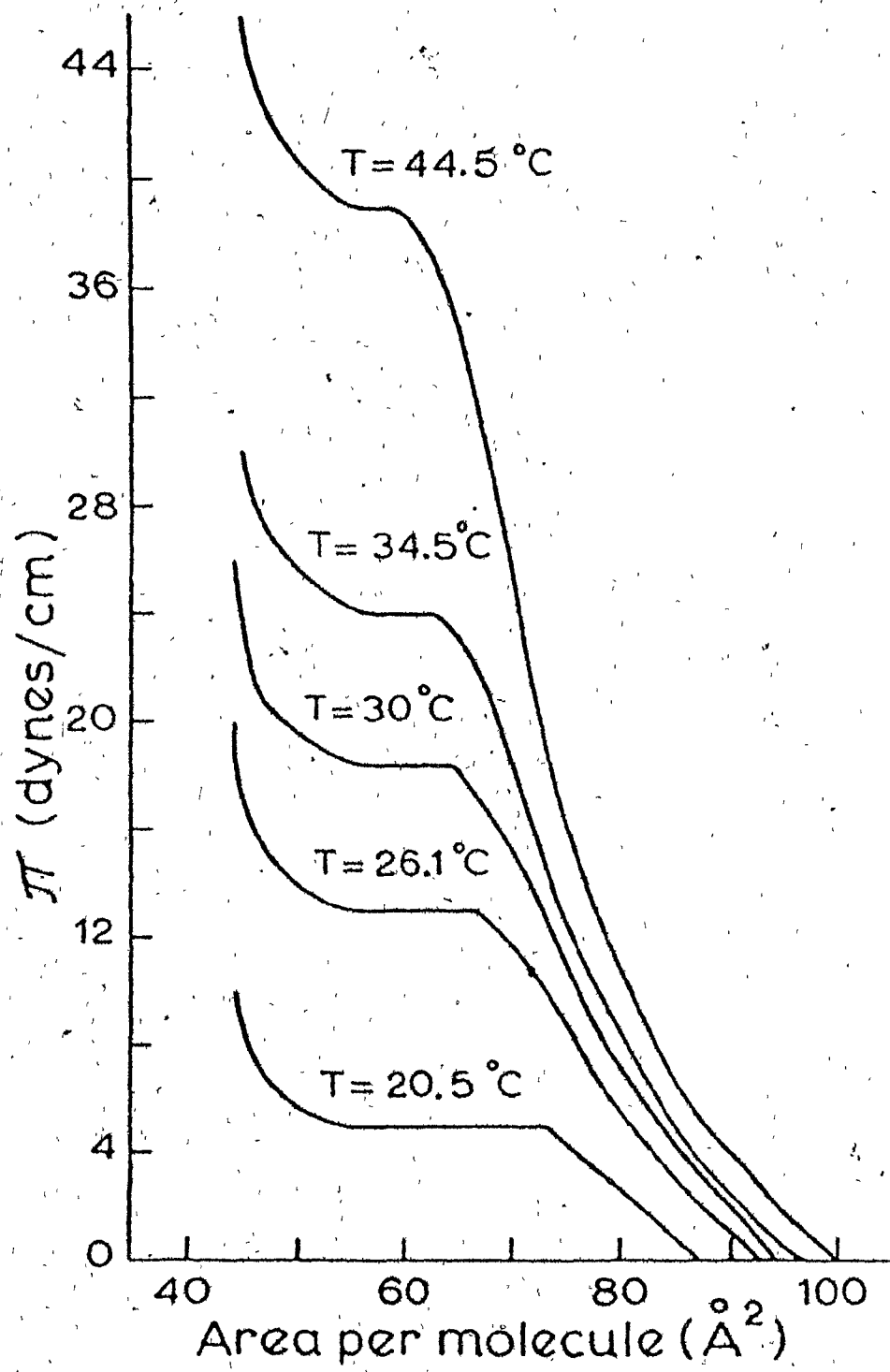


Fig.(4.7) Our final result for the LC/LE phase transition.

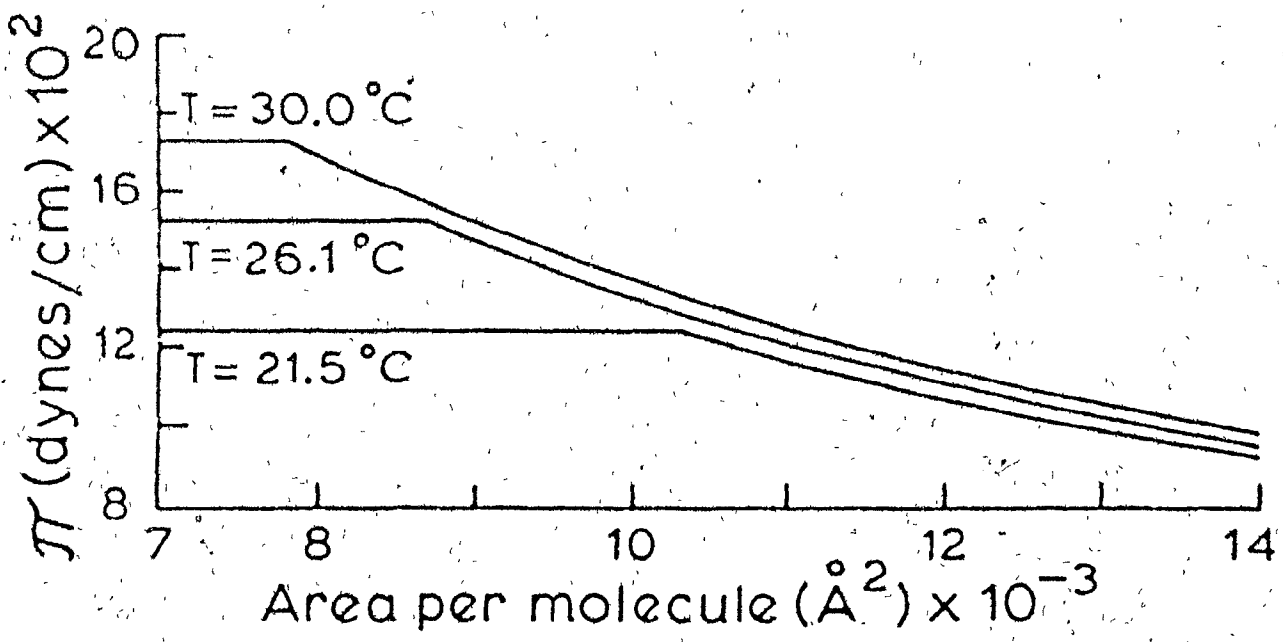


Fig.(4.8) Our final result for the LE/SG phase transition.

CHAPTER V : LC/LE PHASE TRANSITION FOR IMPURE MONOLAYERS

In this chapter we present two mean-field solutions for the LC/LE phase transition for a lipid monolayer with small substitutional impurities. We will focus in particular on β -naphthol as the impurity. The experimental results⁽²⁰⁾ (given in fig.(5.1)) indicate that as the impurity concentration increases, both the LC/LE and LE/SG phase transitions are shifted, broadened and finally eliminated. The film is very much more expanded and fluid. At high pressures, > 30 dynes/cm., the impurity is squeezed out of the monolayer. The impurities are capable of repenetrating the film when the pressure is lowered.

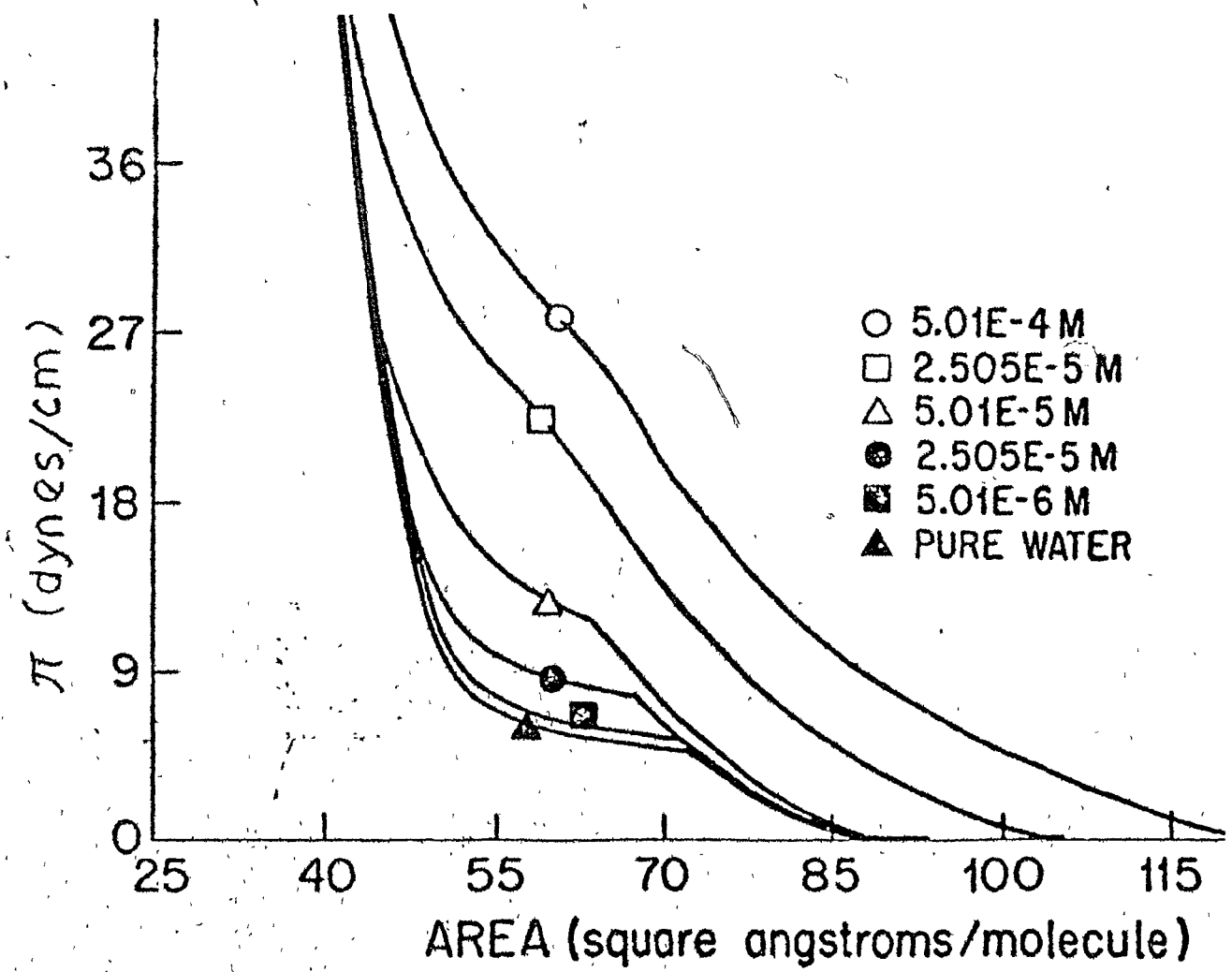
(1) Model for Impure Monolayers:

To the model in chapter II, for the pure lipid system, we now add small substitutional impurities. The general Hamiltonian, considering only nearest neighbour interactions, may be written down in analogy to our previous model, introducing only a new degree of freedom :

$$[S-1] \quad \mathcal{H} = -\frac{J_0}{2} \sum_{\langle ij \rangle} \sum_l \sum_{n,m}^{g,e} J(n,m) \xi_{in} \xi_{jm} + \sum_i \sum_l^{g,e} H(l) \xi_{il}$$

Here ξ_{in} is the generalized site operator introduced in order to distinguish between a lipid chain (l) or an impurity (p). Its values are given as follows : ξ_{ip} takes on the values +1 or 0, depending on whether the i th site is occupied by an impurity or a lipid chain; ξ_{il} may be written as $L_{il}\xi_l$. Here L_{il} is the Lipid chain site operator

Fig.(5.1) DPPC on β -NAPHTHOL substrates : experimental results.



introduced in chapter II. It accounts for the two possible states of the lipid chains, the ground state (g) and the excited state (e). The operator ϵ_{ij} is introduced as a counting device. It takes on the values +1 or 0, depending on whether the i th site is occupied by a lipid chain or an impurity. Furthermore, $-J_0 J(n,m)/2$ represents the, as of yet unspecified, interaction between sites i and j of the lattice occupied by species in state n and m respectively. $H(n)$ denotes the 'magnetic field' or chemical potential associated with the molecular species. If all of the lattice sites are occupied, then :

$$[5-2] \quad \epsilon_{il} \epsilon_{ip} = 1$$

The number of impurities is given by :

$$[5-3] \quad \sum_{ip}^{\text{lattice}} \epsilon_{ip} = \sum_{i=1}^{\text{lattice}} (1 - \epsilon_{ii}) = N_p$$

The Hamiltonian (5-1) may be split into three distinct terms:

$$[5-4] \quad H = H_{ll} + H_{l-p} + H_{pp}$$

where each of the above terms represents the Hamiltonian for the interaction between lipids, a lipid and an impurity and between two impurities, respectively. Expansion of eq.(5-1), elimination of ϵ_{ip} using eq.(5-2), summation over the two possible lipid states, followed by the transformation $Z_{ig} = 1/2(1 + \sigma_i)$, $Z_{ie} = 1/2(1 - \sigma_i)$, with $\sigma_i = \pm 1$, yields the following form for eq.(5-4) :

$$\mathcal{H}_{kk} = \frac{-\tilde{J}}{2} \sum_{ij} \sigma_i \sigma_j \xi_i \xi_j - \tilde{H}(\Pi, T) \sum_i \sigma_i \xi_i$$

$$[5.5] \quad \tilde{J} = \frac{J_0}{4} [J(g,g) + J(e,e) - 2J(e,g)]$$

$$\begin{aligned} \tilde{H}(\Pi, T) = & J_0 q \xi_g [J(g,g) - J(e,e)]/4 \\ & + 1/2 [E_g - E_e + \Pi(A_g - A_e)] - kT \ln(D_e/D_g)/2 \end{aligned}$$

$$\mathcal{H}_{pp} = -\tilde{J}_A \sum_{ij} [\sigma_i \xi_i (1-\xi_j) + \sigma_j \xi_j (1-\xi_i)]$$

$$[5.6] \quad \tilde{J}_A = \frac{J_0}{4} [J(g,p) + J(e,p)]$$

$$\mathcal{H}_{pp} = -\tilde{J}_{AA} \sum_{ij} (1-\xi_i)(1-\xi_j)$$

$$[5.7] \quad \tilde{J}_{AA} = J_0 J(p,p)/2$$

In writing the above equations, we have dropped the constant terms appearing in the Hamiltonians, since these will have no effect on the calculated thermodynamic properties of the system.

In this thesis, we will solve the impurity problem in two different ways. In both cases, we will make use of a mean-field type of assumption, which will replace the site operator ξ_i by its site independent average $\langle \xi \rangle$. This process will be carried out first in the Hamiltonian, then in the partition function.

(ii) MODEL I

In this first method of solution, we will assume that ξ_i may be replaced by its site independent average $\langle \xi \rangle$. We write:

$$[5-8] \quad \langle \xi \rangle = n_1 = N_1 / (N_1 + N_p)$$

$$1 - \langle \xi \rangle = n_2 = N_p / (N_1 + N_p)$$

where N_1 and N_p represent the number of lipid chains and impurities respectively. In this case, our Hamiltonians become :

$$[5-9] \quad \begin{aligned} \mathcal{H}_{I-I} &= \frac{\tilde{J}}{2} \sum_{\langle ij \rangle} \sigma_i \sigma_j - \tilde{H}(H, T) \sum_i \sigma_i \\ \tilde{J} &= \frac{qJ_o}{4} [J(g, g) + J(e, e) - 2J(e, g)] n_1^2 \\ \tilde{H}(H, T) &= J_o q n_1^2 [J(g, g) - J(e, e)] / 4 + n_1 / 2 [H(Ag + Ae) \\ &\quad + (Eg - Be)] - kT \ln(De/Dg)/2 \end{aligned}$$

$$[5-10] \quad \begin{aligned} \mathcal{H}_{I-P} &= -\tilde{J}_A \sum_{\langle ij \rangle} (\sigma_i + \sigma_j) \\ \tilde{J}_A &= \frac{J_o n_1 n_2}{4} [J(g, p) - J(e, p)] \end{aligned}$$

$$[5-11] \quad \begin{aligned} \mathcal{H}_{P-P} &= \tilde{J}_{AA} \sum_{\langle ij \rangle} 1 \\ \tilde{J}_{AA} &= \frac{J_o n_2^2}{2} J(p, p) \end{aligned}$$

These may be further reduced to :

$$[5-12] \quad \begin{aligned} \mathcal{H} &= \frac{\tilde{J}}{2} \sum_{\langle ij \rangle} \sigma_i \sigma_j - \tilde{H}_1 \sum_i \sigma_i \\ \tilde{J} &= \frac{J_o}{4} [J(g, g) + J(e, e) - 2J(e, g)] n_1^2 \\ \tilde{H}_1 &= H(H, T) + J_o n_1 n_2 q [J(g, p) - J(e, p)] / 2 \end{aligned}$$

We see that this Hamiltonian is in exactly the same form as used in

chapter II. Thus, for model I, solving eq.(5-12) on a Cayley tree in the Bethe approximation, will yield exactly the same solutions as presented in chapter II. The effect of the impurities is then to scale the effective interaction energy (J), and to both shift and scale the field (H_1). Thus, as we increase the impurity concentration, we expect the LC/LG phase transition to become washed out and eventually to disappear. Since we explicitly assumed that the distribution of impurities on the lattice is essentially random, we lose the effect of impurity-impurity interactions. Hence, this model will not allow for phase separation or clustering of the impurity.

(ii) Results for Model I

The results for Model I are shown in fig.(5.2). They show that at very low impurity concentrations, the isotherms have the same basic shape as the isotherms for the pure monolayer, except that the transition pressure is shifted towards higher pressures.

Although not illustrated for this model, it was found that for a given concentration of impurities, the interaction between lipids and impurities, J_A , controlled the transition pressure. A positive (repulsive) interaction leads to a depression of the transition pressure towards the transition pressure of the pure monolayer. An attractive (negative) interaction energy has the opposite effect.

A further result of the addition of impurities to the monolayer

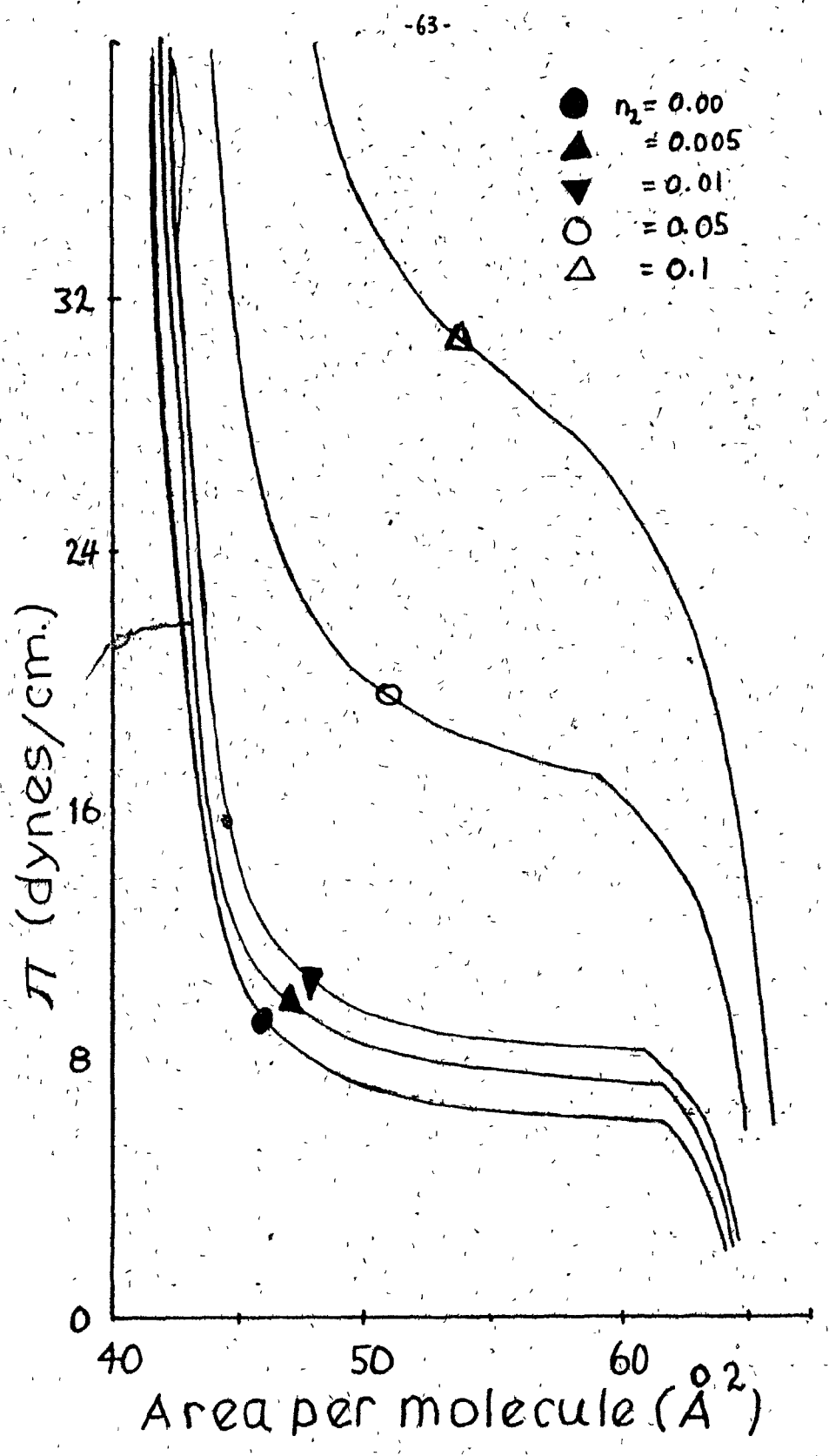


Fig.(5.2)- Results for Model 1 : DPPC with β -naphthol impurities.
 $T = 21.5^\circ\text{C}$; $A_p = 34.0 \text{ \AA}^2$. Full domain structure is included.

system is to make the critical temperature dependent on the impurity concentration :

$$[5-13] \quad Tc^1 = n_1 Tc^0$$

where Tc^0 is the critical temperature of the pure monolayer system; Tc^1 , the new critical temperature. Thus, since $n_1 < 1.0$, the critical temperature will be depressed. This is reflected through the shape of the isotherms with higher impurity concentrations (e.g. $n_1 = 0.1$).

In this thesis, no attempt has been made to model the ejection of the impurity from the monolayer at higher pressures. Thus, our calculated isotherms do not converge onto the isotherms of pure lipid system, as is observed experimentally.

(ii) Model II

In presenting our second model, we will follow a method developed by A. Georgallas⁽³¹⁾. This method is particularly attractive for pseudolattices like the Cayley tree, since it naturally allows the development of higher approximations for the impurity problem. In the equations to follow, setting $n_1 = 1.0$ and $n_2 = 0.0$ allows us to obtain the results for the pure lipid system (i.e. eqs.(2-15,16)). Model II differs from Model I in that we carry out only a partial averaging in the Hamiltonian. We thereby allow for the effect of some nearest neighbour correlations.

Consider now a Cayley tree, whose sites will be filled with either lipid chains or impurities through the addition of successive rings or shells :

(a) If the tree has zero rings, we obtain by inspection :

$$[5.14] \quad Z_{(0)} = 2\cosh(n_1 H)$$

(b) Consider now a Cayley tree with $n=1$ rings. We can write and approximate the Hamiltonians as follows :

$$\begin{aligned} \mathcal{H} &= \tilde{J}_A \sum_j \sigma_0 \sigma_j \xi_0 \xi_j - \tilde{H}(\sigma_0 \xi_0 + \sum_j \sigma_j \xi_j) - J_{AA} \sum_j (\xi_0 - \xi_j)(1 - \xi_j) \\ &\quad - \tilde{J}_A \sum_j (\sigma_0 \xi_0 (1 - \xi_j) + \sigma_j \xi_j (1 - \xi_0)) \\ &\approx [-\tilde{J}_A \sum_j \sigma_0 \sigma_j \xi_j - \tilde{H}(\sigma_0 + \sum_j \sigma_j \xi_j) - \tilde{J}_A \sum_j \sigma_0 (1 - \xi_j)] n_1 \\ [5.15] \quad &+ [-(\tilde{J}_A + \tilde{H}) \sum_j \sigma_j \xi_j - \tilde{J}_{AA} \sum_j (1 - \xi_j)] n_2 \end{aligned}$$

The partition function may now be calculated using :

$$[5.16] \quad Z_{(1)} = \sum_{\{\sigma\}} \exp(-\beta \mathcal{H})$$

For ease of notation, we introduce the convention that coupling constants without a tilda will denote the constant divided by kT (i.e. $J = \tilde{J}/kT$, etc.).

If there is a lipid in the ground state at the origin of the Cayley tree, then :

$$[5.17] \quad Z_{(1)}^{(g)} = \exp[J \sum_j \sigma_j \xi_j + H(1 + \sum_j \sigma_j \xi_j) + J_A \sum_j (1 - \xi_j)]$$

$$= (x + x^{-1})^q \exp[H + qn_2 J_A]$$

where $x = \exp[n_1 H - n_1 J]$

If the lipid chain at the origin of the Cayley tree is in its excited state, then :

$$\begin{aligned} [5-18] \quad z_{(0)}^{(e)} &= \exp\left[-J \sum_j \sigma_j \xi_j + H(-1 + \sum_j \sigma_j \xi_j) - J_A \sum_j (1 - \xi_j)\right] \\ &= (y + y^{-1})^q \exp[-(H + qn_2 J_A)] \end{aligned}$$

where $y = \exp[n_1 H - n_1 J]$

If there is an impurity at the origin :

$$\begin{aligned} [5-19] \quad z_{(0)}^{(p)} &= \exp[(J_A + H) \sum_j \sigma_j \xi_j + J_{AA} \sum_j (1 - \xi_j)] \\ &= [2 \cosh(H + J_A)]^{qn_1} \exp[qn_2 J_{AA}] \end{aligned}$$

The partition function for the Cayley tree with $n=1$ rings is then:

$$\begin{aligned} [5-20] \quad z_{(1)} &= [z(g) + z(e)]^{n_1} [z(p)]^{n_2} \\ &= [\text{Tr } X^q \exp[H + qn_2 J_A] + \text{Tr } Y^q \exp[-(H + qn_2 J_A)]]^{n_1} \\ &\quad \cdot [2 \cosh(H + J_A)]^{n_1 n_2 q} \exp[qn_2^2 J_{AA}] \end{aligned}$$

where the matrices X_1 and Y_1 have been introduced in analogy to the transfer matrices. They are defined to be :

$$[5-21] \quad X_1 = \begin{pmatrix} x & x \\ x^{-1} & x^{-1} \end{pmatrix} \quad Y_1 = \begin{pmatrix} y & y \\ y^{-1} & y^{-1} \end{pmatrix}$$

Each of these matrices has one eigenvalue which is zero. Calling the non-zero eigenvalue $\{\lambda_1, \mu_1\}$ respectively, the parameters (A_1, p_1) may be introduced through the substitutions :

$$\text{Tr } X_1^q = (\text{Tr } X_1)^q = \lambda_1^q = (x + x^{-1})^q = A_1^q e^{qp_1} \quad [5-22]$$

$$\text{Tr } Y_1^q = (\text{Tr } Y_1)^q = \mu_1^q = (y + y^{-1})^q = A_1^q e^{-qp_1}$$

Then our partition function then becomes :

$$Z_{(1)} = A_1^{qn_1^2} [2\cosh(n_1 H + qn_1(p_1 + n_2 J_A))] [2\cosh(H + J_A)]^{n_1 n_2 q} \cdot \exp[qn_2^2 J_{AA}]$$

(c) Proceeding in similar fashion, we write down the partition function for a Cayley tree with $n=2$ rings :

$$[5-24] \quad Z_{(2)} = [e^{-Hn_1} \tilde{Z}_I^{qn_1} + e^{-Hn_1} \tilde{Z}_{II}^{qn_1} + e^{-Hn_1} \tilde{Z}_{III}^{qn_1}] \tilde{Z}_W^{qn_1}$$

where $\{\tilde{Z}_I, \tilde{Z}_{II}, \tilde{Z}_{III}\}$ are defined through the set of equations :

$$\tilde{Z}_A = (x+x^{-1})^{(q-1)} \exp[(q-1)n_2 J_A] = A_1^{q-1} \exp[(q-1)(p_1 + n_2 J_A)]$$

$$\tilde{Z}_B = (y+y^{-1})^{(q-1)} \exp[-(q-1)n_2 J_A] = A_1^{q-1} \exp[-(q-1)(p_1 + n_2 J_A)]$$

$$\begin{aligned} \tilde{Z}_C &= [\exp[H+J_A] + \exp[-(H+J_A)]]^{(q-1)} \exp[(q-1)n_2 J_{AA}] \\ &= [2\cosh(H + J_A)]^{(q-1)n_1} \exp[(q-1)n_2 J_{AA}] \end{aligned}$$

$$[5-26] \quad \tilde{Z}_I = [x \tilde{Z}_A + x^{-1} \tilde{Z}_B]^{n_1} [e^{J_A} \tilde{Z}_C]^{n_2}$$

$$= A_1^{(q-1)n_1} [x \exp\{(q-1)(p_1 + n_2 J_A)\} + x^{-1} \exp\{-(q-1)(p_1 + n_2 J_A)\}]^{n_1} \cdot \\ \cdot [2 \cosh(H+J_A)]^{(q-1)n_1 n_2} \exp\{-(q-1)n_2^2 J_{AA} + n_2 J_A\}$$

$$(5.27) \quad \tilde{Z}_{II} = [y \tilde{Z}_A + y^{-1} \tilde{Z}_B]^{n_1} [e^{-J_A} \tilde{Z}_C]^{n_2} \\ = A_1^{(q-1)n_1} [y \exp\{(q-1)(p_1 + n_2 J_A)\} + y^{-1} \exp\{-(q-1)(p_1 + n_2 J_A)\}]^{n_1} \cdot \\ \cdot [2 \cosh(H+J_A)]^{(q-1)n_1 n_2} \exp\{-(q-1)n_2^2 J_{AA} - n_2 J_A\}$$

$$(5.28) \quad \tilde{Z}_{III} = [\tilde{Z}_A \exp(H+J_A) + \tilde{Z}_B \exp\{-(H+J_A)\}]^{n_1} [\tilde{Z}_C e^{J_{AA}}]^{n_2} \\ = A_1^{(q-1)n_1} \exp[n_2 J_{AA} + n_2(q-1)J_{AA}] [2 \cosh(H+J_A)]^{(q-1)n_1 n_2} \cdot \\ \cdot [2 \cosh(H+J_A + (q-1)(n_1 p_1 + n_2 J_A))]^{n_1}$$

Introducing the substitutions :

$$x_1 = x \exp\{(q-1)n_1(p_1 + n_2 J_A)\} \\ y_1 = y \exp\{(q-1)n_1(p_1 + n_2 J_A)\}$$

$$(5.29) \quad \text{Tr } X_2^q = \lambda_2^q = A_2^q \exp[qp_2] \\ \text{Tr } Y_2^q = \mu_2^q = A_2^q \exp[-qp_2]$$

$$X_2 = \begin{pmatrix} x_1 & x_1^{-1} \\ x_1^{-1} & x_1 \end{pmatrix} \quad Y_2 = \begin{pmatrix} y_1 & y_1^{-1} \\ y_1^{-1} & y_1 \end{pmatrix}$$

Our partition function for n=2 rings then becomes :

$$[S-30] \quad z_{(2)} = B_1^{q(q-1)} B_2^q [2\cosh(n_1 H + q n_1(p_2 + n_2 J_A))] \exp[q n_2^2 J_{AA}]$$

$$B_1 = A_1^{n_1^2} [2\cosh(H + J_A)]^{n_1 n_2}$$

$$B_2 = A_2^{n_2^2} [2\cosh(H + J_A + (q-1)(n_1 p_1 + n_2 J_A))]^{n_1 n_2} \exp[n_2^2 J_{AA}]$$

(d) We generalize these substitutions for $n=s$ rings on the Cayley tree :

$$[S-31] \quad H_s = H + (q-1)(p_s + n_2 J_A)$$

$$x_s = \exp[n_1 H_s + n_1 J]$$

$$y_s = \exp[n_1 H_s - n_1 J]$$

$$X_{s+1} = \begin{pmatrix} x_s & x_s \\ x_{s-1}^{-1} & x_s^{-1} \end{pmatrix}$$

$$Y_{s+1} = \begin{pmatrix} y_s & y_s \\ y_{s-1}^{-1} & y_s^{-1} \end{pmatrix}$$

All of these matrices have one non-zero eigenvalue which may be written as:

$$[S-32] \quad \text{Tr } X_s^q = (\text{Tr } X_s)^q = \lambda_s^q = (x_{s-1} + x_{s-1}^{-1})^q = A_s^q \exp[q p_s]$$

$$\text{Tr } Y_s^q = (\text{Tr } Y_s)^q = \mu_s^q = (y_{s-1} + y_{s-1}^{-1})^q = A_s^q \exp[-q p_s]$$

From these, one easily obtains :

$$[S-33] \quad e^{2p_s} = \lambda_s / \mu_s = \frac{(x_{s-1} + x_{s-1}^{-1})}{(y_{s-1} + y_{s-1}^{-1})} = \frac{\cosh[n_1 H + (q-1)n_1(p_{s-1} + n_2 J_A) + n_1 J]}{\cosh[n_1 H + (q-1)n_1(p_{s-1} + n_2 J_A) - n_1 J]}$$

$$A_s^2 = \lambda_s \mu_s = (x_{s-1} + x_{s-1}^{-1})(y_{s-1} + y_{s-1}^{-1})$$

$$= 4 \cosh[n_1 H + (q-1)n_1(p_{s-1} + n_2 J_A) + n_1 J] \cdot$$

[S-34]

$$\cosh[n_1 B + (q-1)n_1(p_{s-1} + n_2 J_A) - n_1 J]$$

We further have the recurrence relation:

$$z_{(n)} = B_1^{q(q-1)^{n-1}} B_2^{q(q-1)^{n-2}} \dots B_n^{q(q-1)}$$

$$\cdot [2\cosh(n_1 B + qn_1(p_n + n_2 J_A))] \exp[qn_2^2 J_{AA}]$$

where $B_1 = A_1^{n_1^2} [2\cosh(B + J_A)]^{n_1 n_2}$

$$[5-35] \quad B_s = A_s^{n_2^2} [2\cosh(B + J_A + (q-1)(n_1 p_s + n_2 J_A))]^{n_1 n_2} \exp[n_2^2 J_{AA}]$$

These recurrence relations may be solved. We define

$$[5-35] \quad z_s = \tanh(p_s n_1) \quad v = \tanh(n_1 J)$$

It may easily be shown :

$$[5-36] \quad z_s = v \tanh(B_{s-1})$$

Algebraic manipulation then yields:

$$[5-37] \quad \frac{z_s}{v} = \frac{(1 + u_A)(1 + z_{s-1})^{q-1} - (1 - u_A)(1 - z_{s-1})^{q-1}}{(1 + u_A)(1 + z_{s-1})^{q-1} + (1 - u_A)(1 - z_{s-1})^{q-1}}$$

where

$$u_A = \tanh(n_1 B + (q-1)n_1 n_2 J_A)$$

In the thermodynamic limit, $s = \infty$, it may be shown that the above

expression reduces to a polynomial of degree q :

$$[5-38] \quad \frac{z}{v} = \frac{(1 + u_A)(1 + z)^{q-1} - (1 - u_A)(1 - z)^{q-1}}{(1 + u_A)(1 + z)^{q-1} + (1 - u_A)(1 - z)^{q-1}}$$

The free-energy is found using :

$$[5-39] \quad F_n = -kT \ln(Z_n)$$

It may be shown that the central site of the Cayley tree has the same 'magnetization' as that calculated by the Bethe approximation. The central site experiences a 'field' given by :

$$[5-40] \quad H_c = H + q(p_s + n_2 J_A)$$

The 'magnetization' or order parameter is obtained by differentiating with respect to the field at the centre site :

$$\langle \sigma \rangle = - \left(\frac{\partial (F_n / kT)}{\partial H_c} \right)_{p_s, T}$$

$$[5-41] \quad \langle \sigma \rangle = n_1 \tanh(H_c n_1)$$

In terms of the order parameter for the pure lipid system, $\langle \sigma \rangle = \frac{(1+v)z}{z+2v}$, our new order parameter $\langle \sigma \rangle$ for the impure monolayer system is:

$$[5-42] \quad \langle \sigma \rangle = n_1 \left(\frac{\langle \sigma \rangle + \tanh(n_1 n_2 J_A)}{1 + \langle \sigma \rangle \tanh(n_1 n_2 J_A)} \right)$$

(iv) Results for Model II

Our results for Model II are shown in the following series of

graphs. As for Model I, no attempt has been made to model the absorption or ejection of impurities from the monolayer at high pressures, or to model the LE phase for the system.

The variation of the calculated isotherms for a given impurity concentration with respect to the lipid-impurity interaction is illustrated in fig.(5.3). As in the case of Model I, an attractive interaction pushes the isotherms towards higher pressures; a repulsive interaction energy depresses the transition pressures.

In contrast to Model I, the critical temperature depends only linearly on the impurity concentration:

$$[5.43] \quad T_c^1 = n_i T_c^0$$

where T_c^0 is the critical temperature of the pure lipid system, T_c^1 , of the impure system. Thus, although the transition temperature is depressed, it changes only slowly when compared with that of Model I.

Therefore, the isotherms retain their basic shape, even at relatively high impurity concentrations. A comparison of the two models is given in fig.(5.4).

Our 'best fit' to the experimental results is illustrated in fig.(5.5). The system can best be modelled with a weak repulsive interaction between the lipids and impurities. These isotherms also illustrate the full domain structure, in contrast to a single domain as shown in the previous 3 graphs. Attempting to fit the points halfway

across the transition, $A = 55\text{A}^2$, show that the model is successful for low impurity concentrations, but not at higher impurity concentrations. Presumably, at high concentrations, impurity-impurity interactions become important. Our model does not account for these.

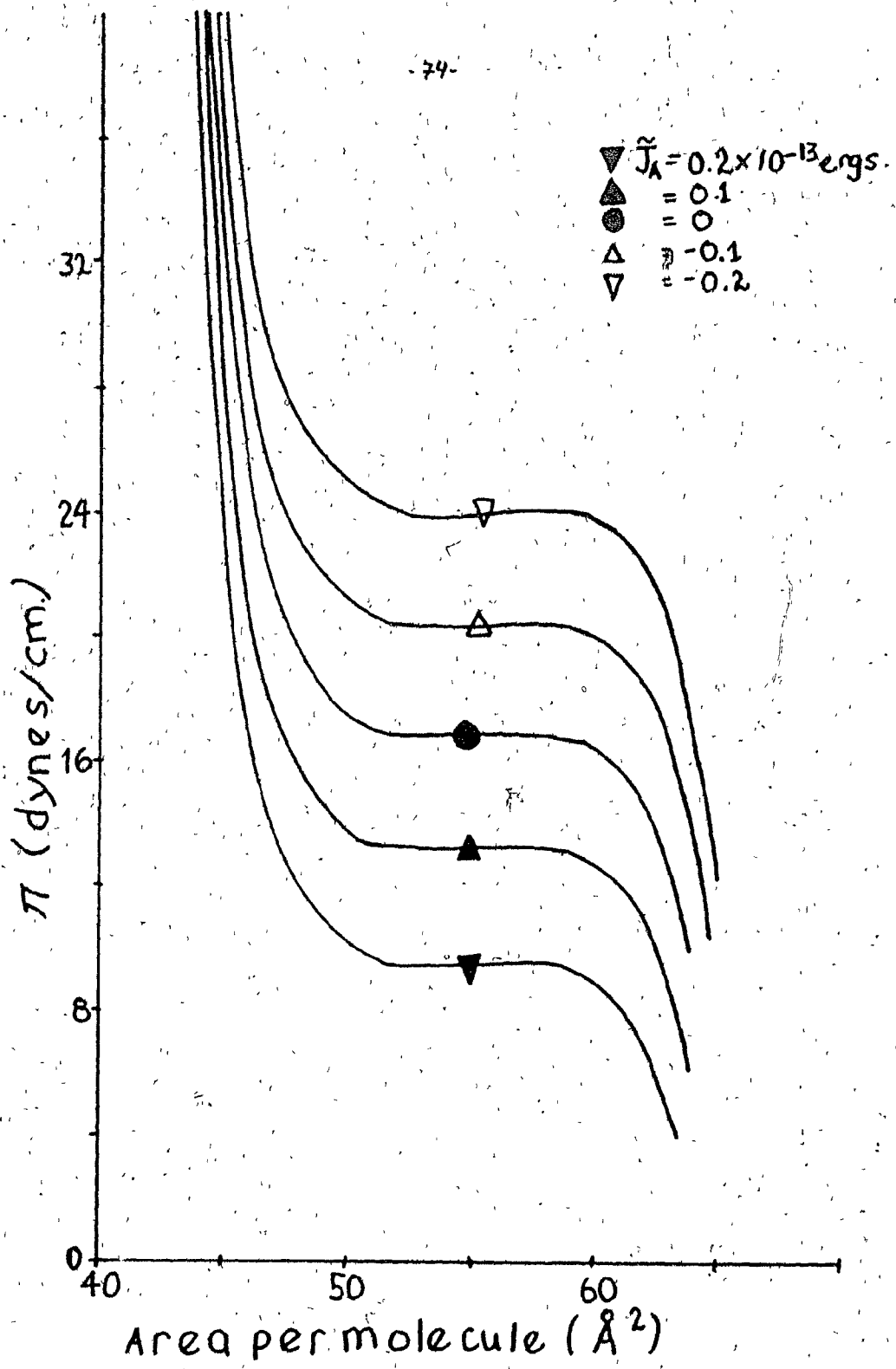


Fig.(5.3) A comparison between isotherms with different impurity-lipid interaction. $T = 21.5^\circ\text{C}$ $A_p = 34.0 \text{ } \text{\AA}^2$ $n_2 = 0.05$.

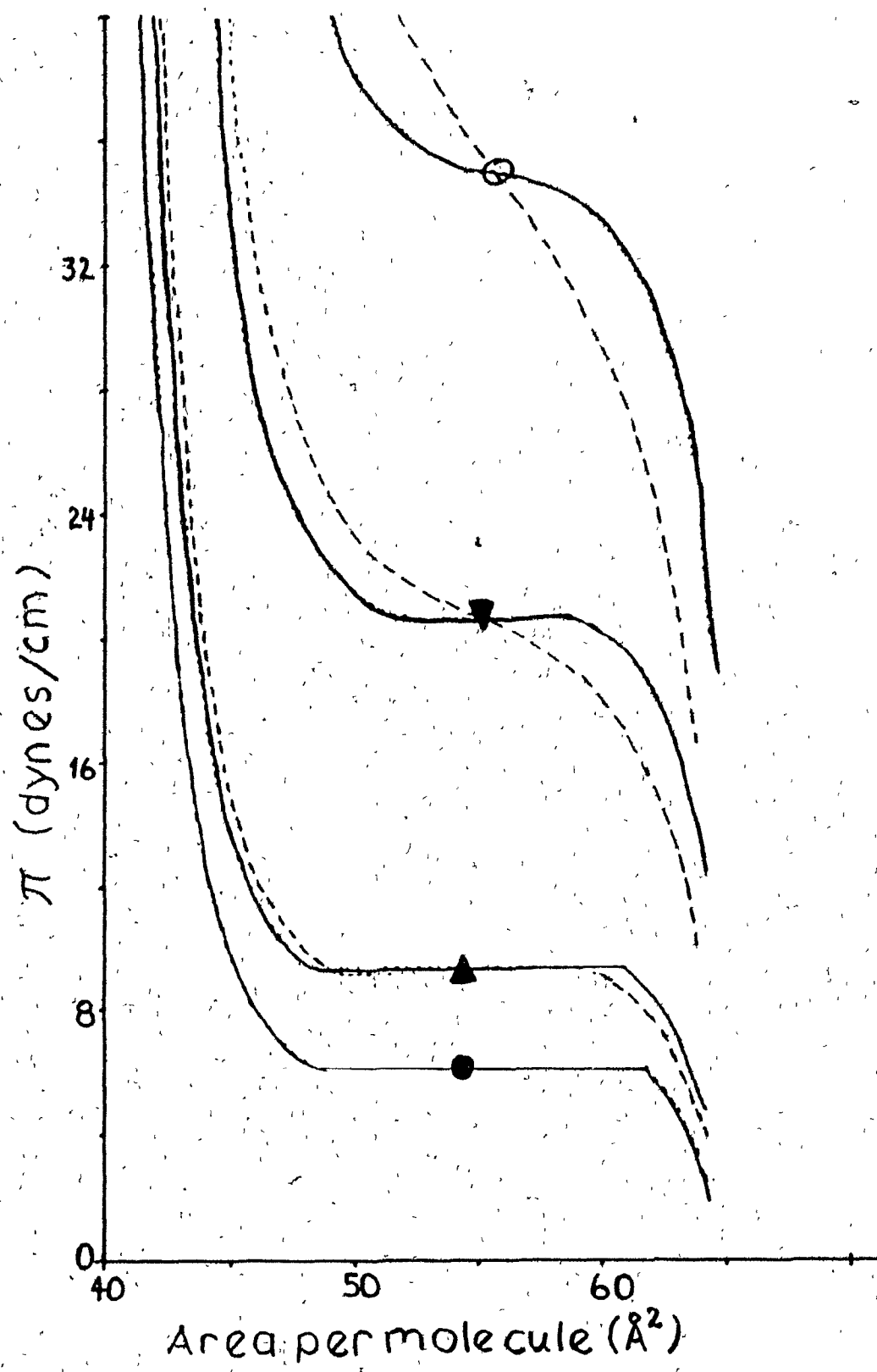


Fig.(5.4) A comparison between the 2 Models. The isotherms are for a single domain at $T = 21.5^\circ\text{C}$; $A_p = 34.0 \text{ } \text{\AA}^2$; $J_A = 0.01 \times 10^{-13}$ ergs..
 ● $n_2 = 0.0$; ▲ $n_2 = 0.01$; ▽ $n_2 = 0.05$; ○ $n_2 = 0.1$.

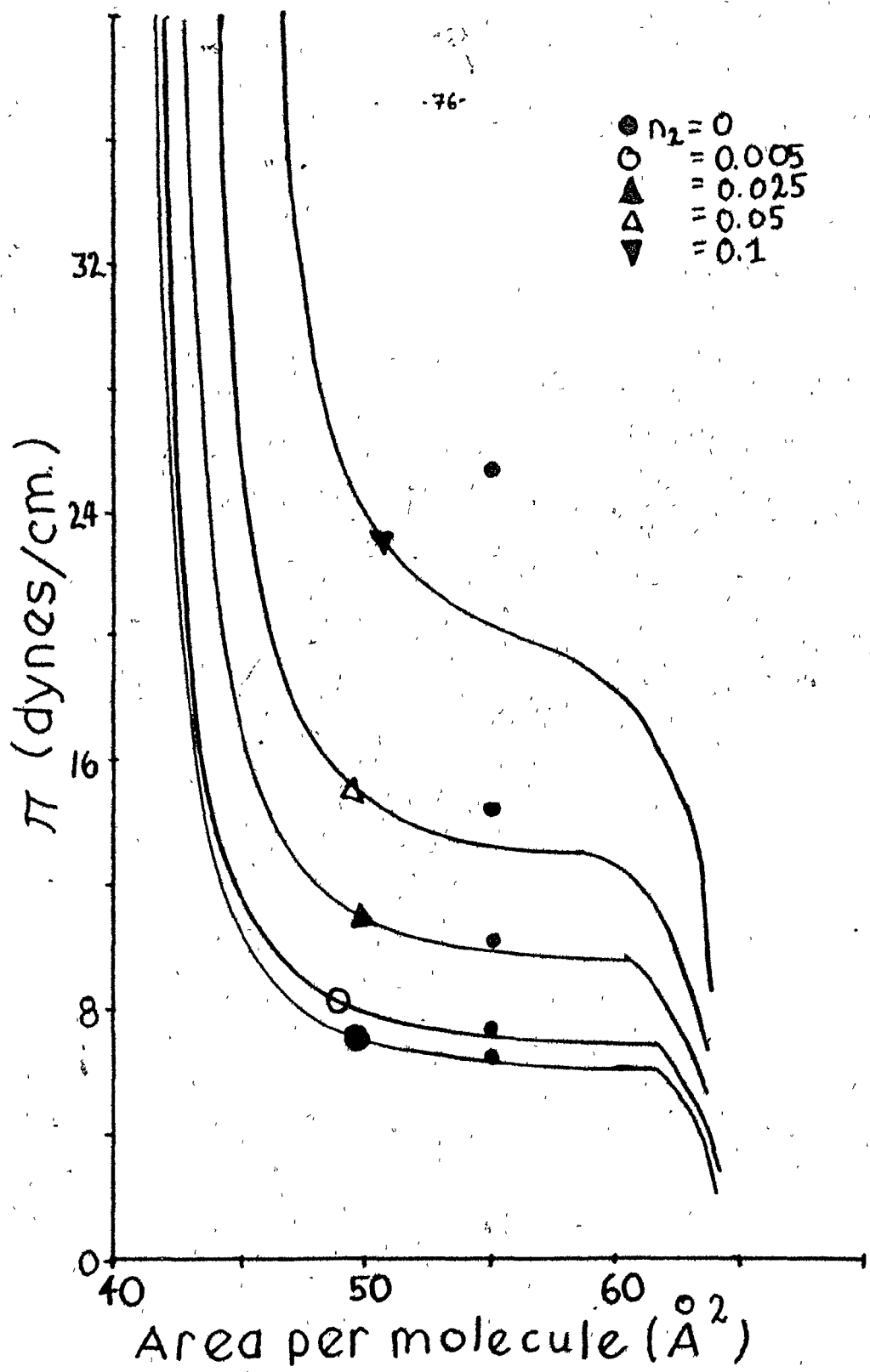


Fig.(5.5) Isotherms generated through Model 11 showing full domain structure. $T = 21.5^\circ\text{C}$; $A_p \approx 34.0 \text{ } \text{\AA}^2$; $J_A = -0.1 \times 10^{-13} \text{ ergs}$. The shaded circle at $55 \text{ } \text{\AA}^2$ indicates the experimental point.

CHAPTER VI : CONCLUSIONS

In this final chapter, we briefly present some possible improvements and extensions to our model, and summarize our conclusions.

The model presented for the complete II - A isotherms of the lipid monolayer is essentially a two-state model in terms of chain orientation with respect to the aqueous substrate. The hydrocarbon chains are in either their upright (the upright chains may be in either their ground or excited states) or 'fallen state'. No attempt has been made to address the dynamics of this collapse. It is likely that this collapse or 'lifting up' of the acyl chains takes place in stages, each of which would have its own interaction energy and statistics. Inclusion of such intermediate states may well result in improved quantitative agreement with the experimental results.

Furthermore, in calculating the statistics for configurations of collapsed chains, molecules with upright chains and vacancies, on our triangular lattice, we treated each chain as being completely separate and independent. This makes our model really more appropriate for single-chained molecules such as soaps. Indeed, for such systems the pressures obtained are in very good agreement with those obtained through experiment. However, in the case of phospholipids such DPPC, there are always two chains per molecule, which are coupled via their glyceride backbone. Thus, our calculations for the entropic terms contributing towards the free energy of the system is really only an

approximation and can possibly be improved.

The treatment of the problem of impure monolayer systems may be extended in numerous ways. In this thesis we presented a model which is strictly for the LC/LE phase transition. Through the introduction of vacancies, the collapse of acyl chains and a proper treatment of the interaction between impurities and lipids, our model could be extended to the LE phase and LE/SG phase transition.

Our treatment of the LC/LE transition for impure monolayers explicitly made use of a mean-field type of assumption on the distribution of impurities on the Cayley tree. Using the method outlined in chapter V, it becomes easy to develop higher approximations for the problem. Such a treatment would entail working with the grand canonical partition function, to explicitly consider all possibilities at each lattice site (i.e. impurity, or lipid chains in ground or excited state) and using the constraint that the number of impurities is fixed as a boundary condition. It is hoped that such improved approximations allow for the possibility of impurity-impurity interactions, and can therefore be used to model situations where phase separation and clustering of the impurities take place.

In his study of impure monolayers using β -naphthol, Cadenhead et al.⁽²⁰⁾ noticed that at high pressures (> 30 dynes/cm.) the impurity was ejected from the lattice. It was originally hoped that such effects could be modelled through an ansatz, which is linear in the order

parameter, similar to eq.(2.13) (here the concentration of the impurity would replace N, the size of the growing lipid domain). Implementation of such a model showed that such a linear ansatz is too simple minded and hence it is not sufficient to model this effect. A more systematic investigation of the absorption is needed.

In calculating $\{N_{\alpha\beta}\}$ in chapter II for the LE phase, we made use of work by Cotter-Martire⁽³⁹⁾. They dealt with a system of rods and solutes. It would be interesting to extend this work, to include the possibilities of vacancies and impurities.

In conclusion, we have presented a model for the phase transitions of lipid monolayers on an air-water interface, which achieves some measure of both qualitative and quantitative agreement with the results obtained experimentally. Our model is based on the following ideas :

(i) The LC/LE phase transition is a chain disordering transition in which the chains go from a rigid, all-trans configuration in the LC phase to a chain melted, excited state in the LE phase. This transition is further modified through the growth of noninteracting, finite-sized lipid domains in the LC phase.

(ii) In the LE phase, the monolayer expands through the introduction of vacancies or holes, and through the collapse of the lipid chains onto the aqueous substrate.

(iii) The LE/SG phase transition is a first-order phase transition.

We have modelled this transition as being driven by the interaction

between the polar head groups of the lipids.

(iv) There seems to be little interaction between lipids in the SG phase. The observed isotherms converge onto those generated by a two-dimensional ideal gas.

(v) Addition of small, substitutional impurities to our lipid system has the effect of shifting, scaling and eliminating the LC/LE phase transition.

and the physical condition of the soil, and
the other section of the soil, and
the depth of penetration placed here.

1000 ft. results -
1000 ft. results -

1000 ft. results -

1000 ft. results -

1000 ft. results -

1000 ft. results -

1000 ft. results -

1000 ft. results -

1000 ft. results -

1000 ft. results -

1000 ft. results -

1000 ft. results -

1000 ft. results -

1000 ft. results -

1000 ft. results -

1000 ft. results -

1000 ft. results -

1000 ft. results -

1000 ft. results -

1000 ft. results -

1000 ft. results -

1000 ft. results -

1000 ft. results -

1000 ft. results -

1000 ft. results -

1000 ft. results -

1000 ft. results -

displacement is to be taken by the soil.
Given the necessary parameters this equation can be solved
for the displacement value.

Another result obtained is

that a greater load will cause a greater displacement.

This is true for all soils.

It is also true for all materials.

It is also true for all materials.

It is also true for all materials.

be dropped from the model. The first two terms in the equation will be dropped because they do not contribute much to the behavior of the system, especially for the experiments at higher frequencies.

The last term in the equation is also dropped because it is not significant in the system. The last term is the error term, which is the difference between the measured value and the calculated value.

The last term in the equation is also dropped because it is not significant in the system. The last term is the error term, which is the difference between the measured value and the calculated value.

The last term in the equation is also dropped because it is not significant in the system. The last term is the error term, which is the difference between the measured value and the calculated value.

The last term in the equation is also dropped because it is not significant in the system. The last term is the error term, which is the difference between the measured value and the calculated value.

The last term in the equation is also dropped because it is not significant in the system. The last term is the error term, which is the difference between the measured value and the calculated value.

The last term in the equation is also dropped because it is not significant in the system. The last term is the error term, which is the difference between the measured value and the calculated value.

The last term in the equation is also dropped because it is not significant in the system. The last term is the error term, which is the difference between the measured value and the calculated value.

The last term in the equation is also dropped because it is not significant in the system. The last term is the error term, which is the difference between the measured value and the calculated value.

The last term in the equation is also dropped because it is not significant in the system. The last term is the error term, which is the difference between the measured value and the calculated value.

The last term in the equation is also dropped because it is not significant in the system. The last term is the error term, which is the difference between the measured value and the calculated value.

The last term in the equation is also dropped because it is not significant in the system. The last term is the error term, which is the difference between the measured value and the calculated value.

The last term in the equation is also dropped because it is not significant in the system. The last term is the error term, which is the difference between the measured value and the calculated value.

The last term in the equation is also dropped because it is not significant in the system. The last term is the error term, which is the difference between the measured value and the calculated value.

The last term in the equation is also dropped because it is not significant in the system. The last term is the error term, which is the difference between the measured value and the calculated value.

ט' כב' ב' ט' ט' ט'

四

卷之三

卷之三

卷之三

二
三
四

לעומת הכתובים במקרא, שפה זו לא הייתה בשימושם.

卷之三

卷之三

卷之三

卷之三

卷之三

卷之三

卷之三

卷之三

ט' ט' ט'

卷之三

卷之三

ה'ג

MEMO ON FORMER CONVENT

PRO-44


```

    .eq=20.45
    .se=24.55
    .no=100.00
    xns=1000000000.00
    xx=-0.01
    xj=x+1.00*x-2.00*xj)/4.00
    vvg=2.00*xvg
    vg=det*xg-dev*xvvg/(dev*xvg+dev*(-vvg))
    hc=x*tc.d0*i/1.00
    hc=nc*(ee-eq)/2.00-xxkt*dp/de/dg/2.00
    sigma=1.00

calculate the levic transition
ij=1
xrd=x+1.00*xns-nc*1.00*sigma
wr=dlog((4.00*xnd-1.00)/0.00)/dlog(5.00)
nr=if(i,wr)
rg=hc+pt*ee-eq/2.00
aa=nc*xvt
pr=dev*xaa-dev*xna/(dev*xaa+de*xra)
c=0.00*pt
c2=0.00*c
z1=1
nc=0.00
r=0.00
zz=1.00
zz=2.00
zz=vg*xj+(1.00*x-1.00)**nv-4.00*(1.00-x-1.00)**nv
zz=k=zz+(1.00*x-1.00)**nv-4.00*(1.00-x-1.00)**nv
pont=0.00
if(z1>0) goto 100
sigma=1.00*sqrt(2.00)*sqrt(2.00)*sqrt(2.00)
if(z1>0) goto 100
format "DO CONVERGENCE OF %1.0 SIGMA"
cc=0.00
if(dabs(sigma-sigma1)<0.1.00001 goto 100
sigma=sigma1
cc=0.00
abc=abc-pt*ee-eq/2.00
vgca=1.00*xvt-abc
ptc=0.00

if past the transition
it=1
ip=0.50
it=0.50,0.00 goto 20
ig=-0.0060
izgx=x*ig+(1.00*xg)+4.00*(1.00*x-1.00)*vg*x
izgy=x*ig+(1.00*xg)+4.00*(1.00*x-1.00)*vg*x
it=100
if(it>it,1000 goto 30)
write(108,108)
format "DO CONVERGENCE FOR %1.0"
ibts=0
if(dabs(ig-ig)/it,0.00001) goto 30
ig=0.00
ibts=20
sigma=ig+(1.00*xg)+4.00*xvg*x
abc=abc*2
abc=abc+abc*ig*vg*x/2.00
xka=abc
vgca=1.00*xvt+1.00*xg+4.00*xvg*x
vgca=1.00*xvt+1.00*xg+4.00*xvg*x
p=1000.00+0
return
end

```

ପରିବାର ପରିବାର ପରିବାର ପରିବାର

THE EMBODIMENT OF CONSCIOUSNESS / Through a bisecting method as before

Implicit 2000+3600=20000.00. get 20

卷之三

卷之三

卷之三

16. *State v. S. L. B.*, \$3000. note 23

卷之三

卷之三

卷之三

卷之三

卷之三

卷之三

卷之三

四
卷之三

100

卷之三

卷之三

200

卷之三

卷之三

卷之三

卷之三

卷之三

卷之三

卷之三

REFERENCES

1. J.Baret , Prog. in Surface and Membrane Sci. 14 (1981).
2. L.Rothfield (editor) , "Structure and Function of Biological Membranes", (Academic Press, New York 1971).
3. M.C.Phillips, D.Chapman, Biochim. Biophys. Acta 163 (1968) p.301.
4. D.Pink,A.Georgallas, M.J.Zuckermann, Z. Physik B 40 (1980) p.103.
5. A.Georgallas, D.L.Hunter, T.Lockmann, M.J.Zuckermann, D.Pink, Eur. Biophys. J. 11 (1984) p.78.
6. Lehninger, "Biochemistry", (Worth Pub., New York ,1970).
7. W.Hoppe, W.Lehmann, H.Markl, H.Ziegler (editors), "Biophysics", (Springer-Verlag, Berlin,1983).
8. D.Cadenhead, Ind. Eng. Chem. 61 (1969) p.22.
9. T.Miyaska, T.Watanabe, A.Fujishima, K.Honda, J.Am.Chem.Soc. 100 (1978) p.6657.
10. A.Caille; A.Rapini, M.J.Zuckermann, A.Cros, S.Doniach, Can. J. Phys. 56 (1978) p.348.
11. A.Caille, D.Pink, F.de Verteuil, M.J.Zuckermann,

- Can. J. Phys. 58 (1980) p.581.
12. O.Albrecht, H.Gruler, E.Sackmann, J.Physique 39 (1978) p.301.
13. N.Gerschfeld, K.Tajima , J. Coll. Inter. Sci.
59 (1977) p.597.
14. M.J.Zuckermann, D.Pink, M.Costas, B.C.Sanctuary,
J. Chem. Phys. 76 (1982) p.4206.
15. N.Pallas, Phd. Thesis, Clarkson Uni: Potsdam N.Y., (1983).
N.Pallas, B.A.Pethica, Langmuir 1 (1985) p.509.
16. M.W.Kim, D.Cannell, Phys. Rev. A 13 (1976) p.411.
17. G.Benedek, G.A.Hawkins, Phys. Rev. Lett. 32 (1974) p.524.
18. N.Gerschfeld, R.Pagano, J. Phy. Chem. 76 (1972) p.1231.
19. H.Doefler, W.Rettig, Coll. & Polymer Sci. 258 (1980) p.415.
20. A.Cadenhead, preprint.
21. M.Loesche, H.Moehwald, Eur. Biophys. J. 11 (1984) p.35.
22. A.Georgallas, D.A.Pink, Can. J. Phys. 60 (1982) p.1678.
23. L.D.Landau and E.M.Lifshitz, "Statistical Physics : Part 1",
(3rd ed.,Pergamon Press, 1980).
24. J.Firpo, These de Doctorat, Uni. de Provence, (1981).

25. J.Firpo, J.Dupin, G.Albinet et al., Phys. Rev. A
22 (1978) p.2782.
26. J.Dupin, J.Firpo et al., J. Chem.Phys. 70 (1979).
27. D.A.Pink, A.Georgallas, J. Coll. Inter. Sci. 89 (1982) p.107.
28. S.Marcelja ,Biochim. Biophys. Acta. 367 (1974) p.165.
29. S.Marcelja , Biochem. Biophys. Acta. 445 (1976) p.1.
30. A.Wulf, J. Chem. Phys. 67 (1977) p.2254.
31. A.Georgallas, Phd. Thesis Uni. of London , (1979).
32. A.Fischer, E.Sackmann , J. Physique 45 (1984) p.517.
33. M.Fisher, S.Ma, A.Nickel, Phys. Rev. Lett. 29 (1972) p.524.
34. T.Smith , J. Coll. Inter. Sci. 23 (1978) p.27.
35. L.E.Reichl, "A Modern Course in Statistical Mechanics ",
(Uni. Texas Press, 1980).
36. N.Gershfeld, J. Coll. Inter. Sci. 32 (1970) p.167.
37. T.Hill, "Introduction to Statistical Mechanics ",
(Addison-Wesley,1960).
38. R.DiMarzio, J.Chem. Phys. 35 (1961) p.658.
39. M.Cotter, E.Martire, J. Mol. Cry. & Liq. Cry. 7 (1969) p.295.

40. Domb,Green (eds), "Phase transitions and Critical Phenomena"
Vol.2, (Academic Press ,New York , 1972).

41. S.Katsura, M.Takizava, Prog. Theor. Phys. 51 (1974) p.84.

42. V.von Tscharner, H.McConnell, Biophys. J. 36 (1982) p.409.

43. G.Albinet, A.-M.S.Tremblay, Physical Rev. A 27 (1983) p.2206.

J.-P.Kegre, G.Albinet, J.-L.Firpo, A.-M.S.Tremblay,
Physical Rev. A 30 (1984) p.2720.

(and references therein)

44. R.M.Weiss, H.M.McConnell, Nature 310 (1984) p.5972 .

H.M.McConnell, L.K.Tamm, R.M.Weiss, Proc. Natl. Acad.
Sci. USA 81 (1984) p.3249.

45. A.Miller, W.Knoll, H.Moewald, to be published.

46. O.G.Mouritsen, M.J.Zuckermann, private communications (1986).